Investigating the effects of *Bartonella quintana* on the host transcriptional cofactor MAL

Isabelle Douylliez

A thesis submitted to Victoria University of Wellington
in fulfilment of the requirements for the degree of
Master of Science in Molecular Microbiology

Te Herenga Waka – Victoria University of Wellington
2024

Abstract

Bartonella quintana is a Gram-negative facultative intracellular bacterial pathogen that has been infecting humans for more than 4,000 years. Today, *B. quintana* is considered a re-emerging pathogen. The *Bartonella* genus contains many species which infect a wide range of mammals, with each *Bartonella* species highly adapted to one or a few mammalian hosts. In a human host, *B. quintana* can lead to a range of clinical manifestations, including the disease trench fever. *B. quintana* infection can be long-term and asymptomatic but can also be life-threatening. Despite being a widespread ancient pathogen capable of causing serious disease, there are many aspects of *B. quintana* infection that remain poorly characterised.

This project investigated the interaction between *B. quintana* and the host transcriptional cofactor MAL. MAL interacts with the transcription factors SRF and NF-κB to control the expression of hundreds of genes involved in actin, the cytoskeleton, cell motility, and inflammation. There is evidence that *B. quintana* interferes with cellular processes controlled by the MAL/SRF and MAL/NF-κB pathways. *B. quintana* potentially induces cytoskeletal rearrangements and cell migration to disseminate within the host and modulates immune responses to evade the immune system. These effects are thought to be mediated by *Bartonella* effector proteins (Beps), which are injected into host cells via type-IV-secretion systems, as some *B. quintana* Beps have been shown to target cell signalling pathways known to regulate MAL.

To assess whether *B. quintana* affects MAL, I developed tissue culture models that allowed the subcellular localisation of MAL within infected host cells to be visualised using fluorescence microscopy. Since the subcellular localisation of MAL is related to its activity, this can be used as a proxy for activation of the MAL/SRF and MAL/NF-κB pathways. *B. quintana* was found to induce MAL nuclear accumulation in macrophage-like cells, suggesting that *B. quintana* can activate MAL in human cells. The specific mechanisms by which *B. quintana* affects MAL's subcellular localisation and activity were not identified, and I was unable to confirm whether *B. quintana* activates the MAL/SRF pathway or the MAL/NF-κB pathway. However, these data suggest that the subversion of host cell signalling by *B. quintana* involves the transcriptional cofactor MAL. Exploring the interactions between *B. quintana* and host signalling pathways is important in identifying potential targets for the treatment of *B. quintana* infection and in contributing to our understanding of cell biology.

Acknowledgements

Firstly, thank you to my supervisor Dr. Joanna MacKichan. Thank you for your expert guidance, for your invaluable feedback and insights, and for your never-ending support. I could not have wished for a better supervisor.

Secondly, thank you to the rest of the JMAC lab group: Brianna, Francesca, Kae and Zoë. Thank you for the coffee trips, for always being there to celebrate the little and big victories, and for all our unhinged conversations. You are the best lab group there is, and I could not have done it without you.

Thirdly, thank you to everyone in AM304 for all your help over the past few years, especially Danielle for all your advice, pep-talks, and for introducing everyone to squish cubes.

Lastly, to my family and friends, thank you for everything.

Table of Contents

List of Figures

List of Tables

List of Appendix Figures

Abbreviations

ANOVA	Analysis of variance
ABRA	Actin binding Rho-interacting protein
AMP	Adenosine monophosphate
Bep	*Bartonella* effector protein
BID domain	Bep intracellular delivery domain
BSA	Bovine serum albumin
ChIP	Chromatin immunoprecipitation
COMPASS	Complex of proteins associated with Set1
DAPI	4′, 6-diamidino-2-phenylindole, dihydrochloride
DMEM	Dulbecco's Modified Eagle medium
DNA	Deoxyribonucleic acid
ECM	Extracellular matrix
EDTA	Ethylenediaminetraacetic acid
EPEC	*Enteropathogenic E. coli*
FCS	Foetal calf serum
FIC domain	Filamentation induced by cAMP domain
FITC	Fluorescein isothiocyanate
FOV	Field of view
GFP	Green fluorescent protein
GPCRs	G protein-coupled receptors
HAT	Histone acetyltransferase
HEK293T/17 cells	Human embryonic kidney 293T/17 cells
HUVECs	Human umbilical vein endothelial cells
IL-1, IL-6, IL-10	Interleukin 1, 6, and 10
IPTG	Isopropyl β-D-1-thiogalactopyranoside
LB	Lysogeny broth
LPS	Lipopolysaccharide
MAL	Megakaryocytic acute leukemia protein
MKL1	Megakaryoblastic leukemia 1 protein
MOI	Multiplicity of infection
MRTF-A	Myocardin-related transcription factor A
MRTF-B	Myocardin-related transcription factor B
MRTFs	Myocardin-related transcription factors
NF-κB	Nuclear factor kappa-light-enhancer of activated B cells
Omp	Outer membrane protein
PBS	Phosphate buffered saline
PCR	Polymerase chain reaction
PEI	Polyethyleneimine
PMA	Phorbol 12-myristate-13-acetate
PRR	Pattern recognition receptor
QQ plot	Quantile quantile plot
RPM	Revolutions per minute
RPMI	Roswell Park Memorial Institute medium

RTKs	Receptor tyrosine kinases
SAP domain	SAF-A/B, Acinus, PIAS domain
SEM	Standard error of the mean
SH2 domain	Src homology 2 domain
SRF	Serum response factor
T4SS	Type-IV-secretion system
TAE	Tris/acetic acid/EDTA
TE	Tris/EDTA
TGF-β	Transforming growth factor-β
TLR2 and TLR4	Toll-like receptor 2 and 4
TNF-α	Tumor necrosis factor-α
Tris	Trisaminomethane
VEGF	Vascular endothelial growth factor
Vomp	Variable outer membrane protein

Chapter 1 - Introduction

1.1 *Bartonella quintana*

1.1.1 The *Bartonella* genus

Bartonella is a genus of Gram-negative α-proteobacterial intracellular pathogens. There are currently 44 recognised *Bartonella* species, and more continue to be discovered[1]. Bartonellae are transmitted by arthropod vectors and infect mammalian hosts, where they colonise the bloodstream and invade and replicate in red blood cells[2]. It is thought that the *Bartonella* genus evolved from insect symbionts and first began infecting mammals about 60 million years ago[3,4]. Since then, bartonellae have radiated to infect a wide range of host species[5].

A simplified phylogeny of the *Bartonella* genus is shown in Figure 1.1. The genus consists of two groups: *B. apis* with *B. tamiae*, and the eubartonellae. *B. apis* symbiotically colonises the gut of honeybees and *B. tamiae* was recently isolated from the blood of human patients, although many aspects of its pathogenesis have not yet been characterised[6]. Since *B. tamiae*'s genome is closely related to the ancestral genome of *B. apis* and it can cause human diease, *B. tamiae* is thought to represent an intermediate state between an insect gut commensal and a mammalian bloodborne pathogen[6]. The eubartonellae can be further divided into four lineages and *B. australis*[7]. Lineage 2 bartonellae only infect ruminants, but lineages 3 and 4 species can infect a wide range of mammals, with linage 4 being the most speciose of the four lineages[7]. Humans are the resevoir host for *B. bacilliformis*, *B. quintana*, and potentially *B. ancashensis*, which was recently isolated from the blood of a human patient thought to be infected with *B. bacilliformis*[8].

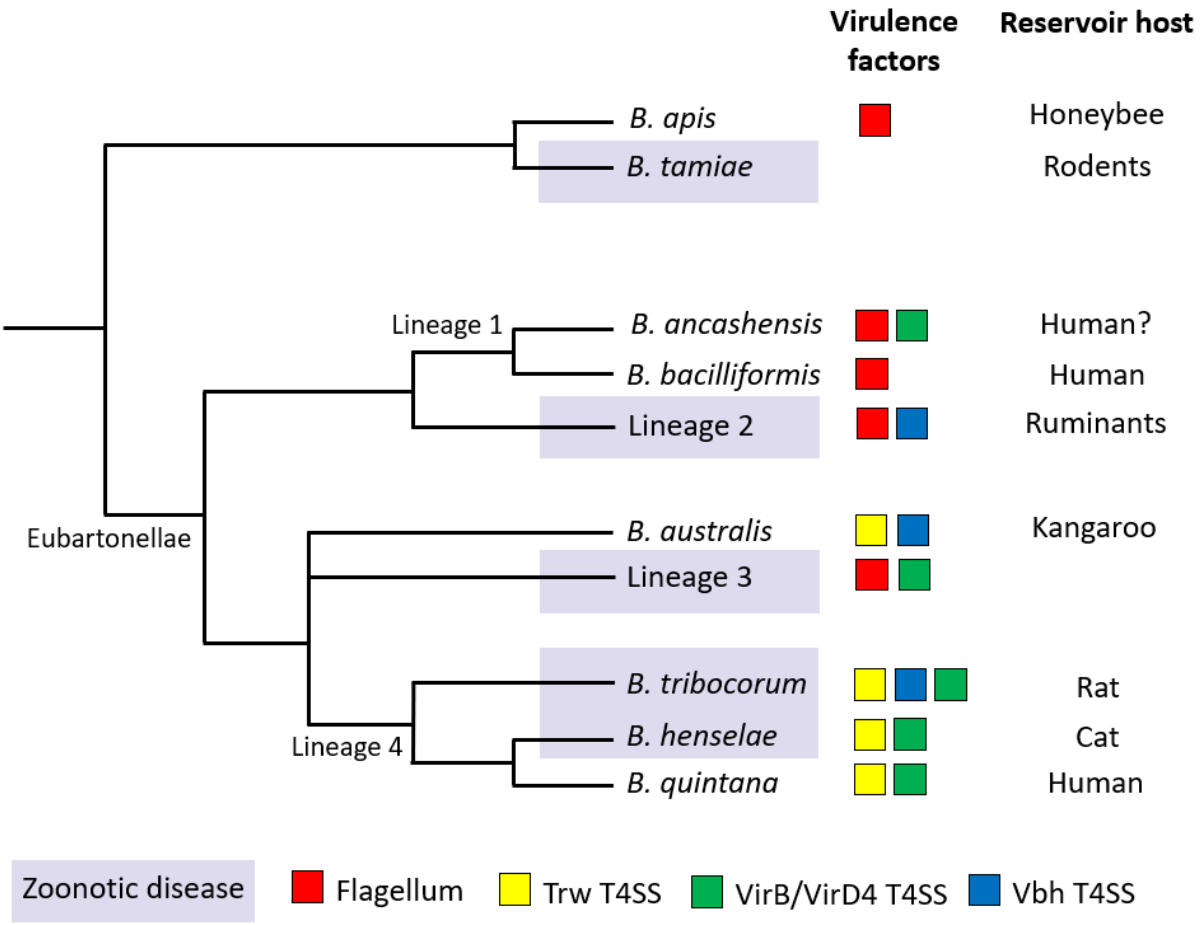

Figure 1.1: Phylogeny of the *Bartonella* genus. This figure is based on a phylogenetic analysis presented in Figure 1 of Wagner and Dehio (2019)[7]. For clarity only some *Bartonella* species are shown, along with their reservoir host and key virulence factors. *B. tamiae*, *B. tribocorum*, *B. henselae*, and some species in lineages 2 and 3 can cause zoonotic disease in humans.

1.1.2 Human bartonellosis

Bartonellosis refers to any human disease resulting from infection by a member of the *Bartonella* genus[9]. Several *Bartonella* species can cause zoonotic infections in humans but most cases of human disease are caused by three species: *B. henselae*, *B. bacilliformis*, and *B. quintana*[10].

B. henselae primarily infects cats, but can cause zoonotic disease in humans that leads to a range of clinical manifestations, including cat scratch disease, bacillary angiomatosis, bacillary peliosis, and endocarditis[11]. Bacilliary angiomatosis is a treatable, but potentially life-threatening, disease that involves angioproliferative lesions in the skin and visceral organs[12,13]. *B. bacilliformis* is a deadly pathogen which causes Carrión's disease and is endemic to the Andes[10]. This was the first *Bartonella* species to be identified, and differs from other bartonellae in that it causes serious disease in its host[10,14]. Whilst both *B.*

bacilliformis and *B. quintana* infect humans as their reservoir host, *B. quintana* is rarely lethal[10,11]. *B. quintana* causes the disease trench fever[11]. Trench fever often involves a high-grade fever, pain in the shins and bones, dizziness, and headaches[9]. In relapsing trench fever, fever attacks occur every five days[15]. Symptoms are very variable, and in some cases *B. quintana* causes a chronic asymptomatic infection[16]. Trench fever is usually self-limiting, and whilst no deaths due to the disease have been reported, infection can last years and result in disability[14]. However, *B. quintana* can also cause bacillary angiomatosis, chronic bacteraemia, and endocarditis, which can be life-threatening, especially in immunocompromised individuals[14].

Trench fever was first decribed in 1915 and is thought to have affected more than 1 million soldiers during WWI[16]. Incidence decreased after the end of WWI, but then increased again during WWII[16]. Trench fever epidemics often occur during times of war, and there is evidence of outbreaks occuring in the Turkish War of 1877-1883 and in the Middle Ages[15]. The recovery of *B. quintana* DNA from ancient dental pulp samples suggests that the bacteria have been infecting humans for at least 4,000 years[17–19]. Currently, *B. quintana* is considered a re-emerging pathogen and mainly affects homeless populations worldwide[20]. Treatment of *B. quintana* infection is limited to the use of antibiotics[20]. Novel treatments which inhibit the specific *B. quintana*-host cell interactions which occur at different stages of its life cycle could improve our ability to treat trench fever and other human bartonelloses.

1.1.3 Infection cycle

The infection cycle of *B. quintana* is similar to that of other bartonellae. *Bartonella* species colonise the gut of their arthropod vectors, which then shed bacteria in their faeces when they take a blood meal from a mammalian host[9]. Lineage 1 and 2 bartonellae are spread by biting Diptera such as sandflies and keds, which damage blood vessels in the skin whilst feeding[21]. This allows the bacteria to pass directly from insect faeces into the host bloodstream. In contrast, lineage 3 and 4 bartonellae are spread by biting arthropods such as fleas, lice, and ticks which do not cause as much damage to the host's skin when feeding[21]. Because they are not directly injected into the bloodstream by their vectors, these *Bartonella* species must travel through the dermis and interact with host cells before reaching the bloodstream[21]. It is thought that by interacting with migratory immune cells such as macrophages and dendritic cells (DCs), *Bartonella* disseminate from the dermis to the lymphatic system, and then to the blood[22,23]. There is evidence that some bartonellae establish a "blood-seeding niche", by invading the endothelial cells lining blood vessels, which allows the bacteria to be

periodically released into the bloodstream, where they invade and replicate in red blood cells[23]. *Bartonella* persist in the blood and infect arthropod vectors when they take blood meals from infected hosts, and thus the cycle of infection continues[24]. This infection strategy requires *Bartonella* to modulate cellular processes in several types of host cells, and in many cases, these effects are mediated by type-IV-secretion systems (T4SSs)[25].

1.1.4 *Bartonella* T4SSs

T4SSs are used by Gram-negative bacteria to transport DNA and proteins across membranes in order to mediate the exchange of DNA with other bacteria and to inject effectors into host cells[2]. Bartonellae use different T4SSs at different stages of their infection cycles[26]. Three different types of T4SSs are found in *Bartonella*: Trw T4SSs, Vbh T4SSs, and VirB/D4 T4SSs[2]. The distribution of these different T4SSs throughout the *Bartonella* genus is shown in Figure 1.1. All eubartonellae except for *B. bacilliformis* encode at least one T4SS[2]. Trw T4SSs do not inject any effector proteins into host cells but are invovled in red blood cell invasion[21]. Flagella are also important for mediating interactions with host red blood cells, and *Bartonella* species that encode genes for the Trw T4SS do not have a flagella, and vice versa[21]. All lineage 4 bartonellae have a Trw T4SS and a VirB/VirD4 T4SS, and some species, such as *B. tribocorum*, also have a Vbh T4SS[7].

Bartonella effector proteins (Beps) are injected into host cells by VirB/VirD4 T4SSs to modulate cellular processes and allow *Bartonella* to establish a successful infection[2]. All Beps, except *B. quintana* BepA1, contain at least one Bep intracellular delivery (BID) domain[27]. This domain is required for translocation via the VirB/VirD4 T4SS, but BID domains can also interact with host cell proteins[24]. Additionally, most Beps contain filamention induced by cAMP (FIC) domains which can AMPylate target proteins, thus altering their function[7].

Whilst some parts of Bep gene sequences are highly conserved, others differ significantly between closely related *Bartonella* species[7]. VirB/VirD4 T4SSs have been acquired three times in the *Bartonella* genus: in lineage 3, lineage 4, and in *B. ancashensis*[26]. Within these three groups of bartonellae, VirB/VirD4 T4SSs and their associated Beps have undergone parallel evolution[28]. Bep genes can undergo gene duplications, and thus can rapidly evolve a diverse range of functions[28]. It is thought that the diversification of Bep sequence and function allowed bartonellae to rapidly radiate to infect many different mammalian hosts, while increasing host-specificity and reducing virulence[2,28].

1.1.5 Bep-host cell interactions

Beps have been shown to modulate a diverse range of cellular processes, including actin rearrangments, cell migration and proliferation, and inflammatory responses[2]. Some Bep-host cell interactions are conserved, whilst others are species-specific. For example, BepA from *B. henselae* and the homologous *B. quintana* protein BepA2 inhibit apoptosis in endothelial human cells, whilst *B. tribocorum* BepA does not[27]. BepC from several *Bartonella* species can induce host cell cytoskeletal rearrangements, suggesting that this effect is important in establishing a successful infection[29]. The BepE protein from different bartonellae can cause human cells to form membrane ruffles, but only *B. quintana* BepE activates host cell autophagy[30].

Whilst many of the molecular interactions between Beps and host cells are not yet fully understood, it is clear that cell migration, immune responses, and cytoskeletal rearrangements are targeted. Therefore, Beps likely target components of signalling pathways which regulate these cellular processes.

1.2 The host transcriptional cofactor MAL

Mammalian cell signalling is complex. Different pathways interact to transduce signals and direct appropriate cellular responses. Megakaryocytic acute leukaemia protein (MAL) is a transcriptional cofactor that responds to several distinct signalling pathways and interacts with transcription factors to regulate gene expression[31,32]. In particular, MAL is important to cell migration, cytoskeletal rearrangements, inflammation, and immunity, which can be affected by *B. quintana*[23,29,33–35].

1.2.1 Myocardin-related transcription factors

MAL, also called megakaryoblastic leukaemia protein 1 (MKL1) or myocardin-related transcription factor A (MRTF-A), is part of a family of transcription cofactors called myocardin-related transcription factors (MRTFs), which include MKL2 (also called MRTF-B) and myocardin[31]. Myocardin is only expressed in cardiac and smooth muscle cells, whilst MAL and MKL2 are widely expressed[31]. MRTFs were first identified for their ability to interact with the transcription factor serum response factor (SRF) and potentiate its effects on gene expression[36]. However, research over the past decades has shown that MAL can also interact with other transcription factors and even have transcription-independent effects, some of which are only beginning to be characterised[32,37].

Myocardin, MAL, and MKL2 can direct different gene expression profiles, and have different effects in different cell types, but share a conserved structure and mechanism of action[36,38]. All contain a SAP (SAF-A/B, Acinus, PIAS) domain which allows them to bind DNA[36]. Via their basic glutamine rich domains, MRTFs bind SRF, thereby recruiting the transcription factor to the promoter of target genes[36]. These domains, and the N-terminal region of MRTFs, are highly conserved across myocardin, MAL, and MKL2[36]. MRTFs also contain RPEL domains (arginine-proline-x-x-x-glutamic acid-leucine repeats, where x is any amino acid) which contribute to their regulation[39].

1.2.2 Regulation of MAL

MAL's activity is regulated, in part, by it subcellular localisation[40,41]. In unstimulated cells, MAL continuously shuttles between the cytoplasm and the nucleus[40]. In response to signals such as serum, the nuclear export of MAL is blocked and MAL rapidly accumulates in the nucleus[40]. MAL's subcellular localisation is regulated by actin dynamics[41]. G-actin binds to MAL via its RPEL domains, and thereby blocks the nuclear localisation signal of MAL, preventing its nuclear import[41]. When not bound to G-actin, MAL can bind importin α/β and move to the nucleus, where it can interact with transcription factors such as SRF and contribute to gene expression[42]. G-actin monomers polymerise to form F-actin filaments[42]. These filaments are continuoulsy assembled and disassembled in response to different signals[43]. For instance, extracellular signals such as TGF-β, serum, and mechanical cues activate Rho GTPases like RhoA, which in turn activate the ROCK and mDia pathways[41,44,45]. ROCK inhibits the depolymerisation of F-actin, whilst mDia promotes the formation of new F-actin filaments[41]. Both of these pathways act to reduce the levels of G-actin in the cytoplasm and release MAL from inhibitory G-actin binding[32]. Processes that reduce the levels of F-actin in the cell result in increased G-actin levels and thereby inhibit the nuclear localisation of MAL[32]. Actin dynamics in the nucleus also contribute to the regulation of MAL, and G-actin binding allows MAL to interact with Crm1 exportin and be exported from the nucleus[39]. In addition, post-translational modifications such as phosphorylation and interactions with other proteins, both in the nucleus and cytoplasm, affect MAL's activity[32,42]. Some of the key factors involved in the regulation of MAL are shown in Figure 1.2.

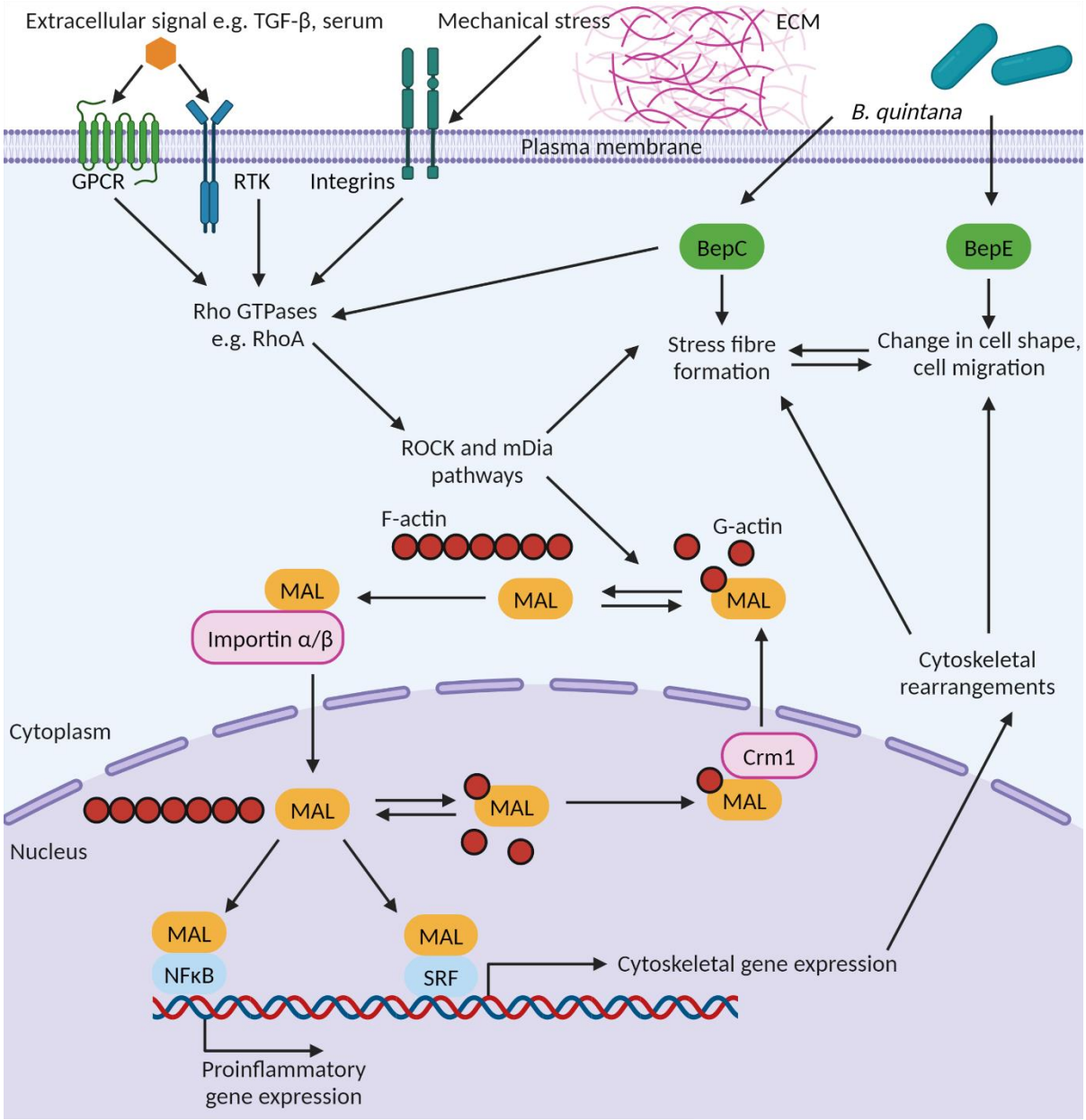

Figure 1.2: The MAL signalling pathway and *B. quintana* Beps. Extracellular signals such as TGF-β, serum, and mechanical changes in the extracellular matrix (ECM) can activate a range of receptors (including but not limited to G protein-coupled receptors (GPCRs), receptor tyrosine kinases (RTKs), and integrins) which in turn activate Rho GTPases, such as RhoA. Rho signalling, via the ROCK and mDia pathways, promotes the formation and stability of F-actin, which releases MAL from G-actin binding. MAL can then be imported into the nucleus by importin α/β where it interacts with transcription factors such as SRF and NF-κB to drive changes in gene expression which contribute to cytoskeletal rearrangements and inflammation, respectively. Binding to G-actin and Crm1 exportin promotes the nuclear export of MAL. The *B. quintana* Beps depicted have been shown to target components of the RhoA/ROCK signalling pathway and cause cytoskeletal rearrangements. Created using Biorender.com (2024).

1.2.3 Effects of MAL

1.2.3.1 The MAL/SRF pathway

MAL can have many effects, however its SRF-dependent effects on gene expression are the best characterised. SRF is a transcription factor which controls the expression of more than 300 genes involved in the actin cytoskeleton, cell migration, and cell structure[46]. The actin cytoskeleton is therefore both a regulator of MAL activity and a target of MAL/SRF signalling[47]. Activation of the MAL/SRF pathway can increase cell proliferation, differentiation, and motility[46,48]. Excessive MAL/SRF signalling contributes to the development of several types of cancer and organ fibrosis[49,50]. In endothelial cells, the MAL/SRF pathway regulates angiogenesis by driving expression of the proangiogenic gene CCN1[51]. This response is regulated by VEGF, which binds cell surface receptors and activates Rho signalling[52]. *Bartonella* species have been shown to modulate angiogenesis and cell proliferation, and this is thought to contribute to the formation of vasoproliferative lesions in diseases such as bacillary angiomatosis[53]. There is also evidence of bartonellae subverting the host actin cytoskeleton, another key target of MAL/SRF signalling[53].

1.2.3.2 Role of MAL in immuntity

MAL can interact with transcription factors other than SRF, such as STAT3, YAP/TAZ and NF-κB[32]. The NF-κB family of transcription factors are involved in inflammation, immunity, cell proliferation, differentiation, and survival[54]. Like MAL, NF-κB can be activated by Rho GTPases such as RhoA, and respond to changes in the actin cytoskeleton[55,56]. NF-κB is a central part of innate and adaptive immune responses, and contributes to the regulation of more than 150 target genes[57]. Some of NF-κB's effects on gene expression require MAL[58]. The MAL/NF-κB pathway is important in directing proinflammatory responses in many types of immune cells, such as macrophages[58]. Although the mechanisms involved have not yet been fully elucidated, LPS and TNF-α can activate MAL, causing it translocate to the nucleus, recruit NF-κB to the promoters of target genes, and mediate epigenetic modifications which lead to the expression of proinflammatory cytokines[58]. It could be that pattern recognition receptors such as TLR4 initiate signalling cascades which interfere with actin the Rho pathway and promote MAL's nuclear localisation. However, MAL is also important in mechanotransduction in immune cells, so could activate the NF-κB pathway in response to mechano-sensitive receptors such as integrins[34]. Regardless of how it is activated, MAL is an essential component of NF-κB-dependent proinflammatory responses in macrophages[59].

In addition, MAL is important in regulating the cytoskeleton of immune cells[33]. MAL deficiency impairs the migration and phagocytic activity of certain types of immune cells, such as neutrophils, which leads to primary immunodeficiencies[60]. MAL also regulates fibroblast migration and cytoskeletal rearrangements in DCs[61]. Macrophages and DCs are migratory immune cells found in dermis, and potentially interact with *B. quintana* during the early stages of infection. These interactions likely involve *Bartonella*-mediated subversions of the host cytoskeleton and immune responses, both of which are regulated by MAL.

1.2.4 Potential interactions between *B. quintana* and MAL

In addition to MAL being a central mediator of many cellular pathways potentially targeted by *B. quintana*, there is also evidence that some bacterial factors, including *Bartonella* Type-IV-secreted effectors, directly interact with cell signalling components that affect MAL. As shown in Figure 1.2, BepE and BepC from *B. quintana* can induce cytoskeletal rearrangments in host cells, such as membrane ruffles, filopodia, and stress fibre formation[29,30]. BepC has been shown to activate RhoA, and BepE apparently activates Rho signalling, by directly or indirectly acting on RhoA or ROCK[23,29]. Multiple effectors from diverse bacterial pathogens have been shown to target Rho GTPases to modulate cellular processes[62,63]. Pathogenic bacteria have also been shown to affect the host cytoskeleton[64]. *Enteropathogenic E. coli* (EPEC) was found to induce the nuclear localisation of MAL in host cells by using the effector protein Tir to activate the Rho signalling pathway[64].

So, whilst many aspects of *B. quintana*-host cell interactions and MAL signalling remain poorly understood, previous research suggests that, similarly to other bacteria, *B. quintana* could target MAL using effector proteins.

1.3 Research aims

The aim of this research project was to determine if *B. quintana* affected the transcriptional cofactor MAL in human cells. Investigating this interaction could help identify the specific cell signalling pathways targeted by *B. quintana*, and the mechanisms by which *B. quintana* establishes a successful infection.

In order to assess the effect of *B. quintana* on MAL, I developed tissue culture models which allowed the subcellular localisation of MAL in human cells to be visualised using fluorescence microscopy. Since the nuclear accumulation of MAL has been shown to

correlate with activation of the MAL/SRF and MAL/NF-κB pathways, this method can be used as a proxy for determining if MAL is activated in response to *B. quintana*.

In the 20 years since its discovery, it has become clear that MAL is a key mediator of several cellular processes. However, many aspects of its regulation, response to different signals, and role in directing different gene expression profiles have not yet been elucidated. Despite being an ancient deadly pathogen, many aspects of *B. quintana*'s infection strategy are also not well understood. Uncovering the interactions between MAL and *B. quintana* could lead to the development of new treatments for bartonellosis, and improve our understanding of cell biology.

Chapter 2 - Materials and methods

2.1 Buffers and solutions

All water was distilled using a HiQ 103s water still and sterilised by autoclaving at 121 °C for 15 minutes. Unless specified otherwise, buffers, solutions, and agar were sterilised by autoclaving at 121 °C for 15 minutes.

2.1.1 Phosphate buffered saline (PBS)

One PBS tablet (Gibco) was dissolved in 500 mL of water and the solution was autoclaved.

2.1.2 Fixative solution

First, separate stock solutions of 0.5 M dibasic sodium phosphate (Sigma-Aldrich) and 1 M monobasic sodium phosphate (Sigma-Aldrich) in water were made. These solutions were stored at room temperature for up to one month. Then, a stock solution of 8% (w/v) paraformaldehyde (Sigma-Aldrich) in water was made. This involved adding the paraformaldehyde to about 80% of the final desired volume of water, adjusting the pH using 2 M NaOH to pH 10 – 12, then heating the solution to 60 °C to dissolve the paraformaldehyde. Once cool, the pH of the solution was adjusted to pH 7.4 using 6 M HCl, and water was added to bring the solution up to the final desired volume. The stock paraformaldehyde solution was stored at 4 °C for up to one month.

Complete paraformaldehyde fixative solution was 2% paraformaldehyde, 60 mM dibasic sodium phosphate, 14 mM monobasic sodium phosphate in water. Once made, fixative solution was filtered using a 0.22 µm membrane filter and stored at 4 °C for up to one week.

2.1.3 Glycerol solutions

Glycerol solutions of various concentrations were made with glycerol (Univar Solutions) and water and autoclaved before use.

2.1.4 Tris/EDTA (TE) buffer

TE buffer was made to a final concentration of 10 mM Tris-HCl (pH 8.5) and 1 mM EDTA (Sigma-Aldrich) in water.

2.1.5 Tris/acetic acid/EDTA (TAE) buffer

To make 1 L of 50× TAE buffer, 242 g of Tris-base (Bio-Rad), 100 mL of 0.5 M EDTA (Sigma-Aldrich) and 57.1 mL of 100% glacial acetic acid (CARLO ERBA Reagents) were made up in water.

2.1.6 Gel electrophoresis

Agarose gels (1%) were made by dissolving 0.6 g of HyAgarose™ (HydraGene) in 60 mL of 1× TAE buffer, and then adding 3 µL of RedSafe™ Nucleic Acid Staining Solution (iNtRON). Gels were poured and allowed to set for at least 15 minutes before covering with 1× TAE buffer and loading. For PCR products and digested plasmids, 10 µL of each sample was mixed with 2 µL of 6× Purple Loading Dye (NEB) or 10 µL of 10% glycerol, and 4 µL of HyperLadder™ 1 kb (Bioline) was included as a DNA ladder. Gels were run at 100 V for 1 – 1.5 hours and imaged under UV light using a Typhoon FLA 9500 scanner (Cytiva). Gel images were edited and analysed using FIJI software[65].

2.2 Bacterial media and culture

All media and solutions were autoclaved at 121 °C for 15 minutes. The bacterial strains used are listed in Table 2.1. *Escherichia coli* strains were used for plasmid maintenance.

Table 2.1: Bacterial strains

Bacterial species	**Strain**	**Plasmid**	**Source**
E. coli	DH5α	pcDNA3 mCherry LIC (6B) (see Table 2.2)	Addgene
E. coli	One Shot™ TOP10	MAL reporter plasmid (see section 2.3.3)	Invitrogen
Bartonella quintana	JK31	None	BEI Resources, NIAID, NIH: *Bartonella quintana*, Strain JK31, NR-31832
GFP-*Bartonella quintana*	JK31	GFP-pSRK plasmid with kanamycin resistance	Joanna MacKichan's lab

2.2.1 LB agar plates

LB agar was made by adding 16 g of LB Agar (Invitrogen) to 500 mL of water and autoclaving the solution. Once the agar had cooled to 50 °C, ampicillin (Sigma-Aldrich) was added to a final concentration of 100 µg/mL. The agar was poured into sterile Petri dishes

and left to set at room temperature with lids slightly ajar. Plates were stored inverted at 4 °C for up to one month.

2.2.2 Chocolate agar plates

To make 1 L of chocolate agar, 36 g of GC agar (Oxoid) and 10 g of bovine freeze-dried BBL™ haemoglobin (BD) were dissolved in 500 mL of water separately and autoclaved. The two solutions were cooled to 45 °C – 50 °C, combined, and supplemented with 1% IsoVitaleX Enrichment Medium (BD), 5 µg/mL vancomycin, 10 µg/mL cycloheximide, and 8 µg/mL amphotericin B (Sapphire Bioscience). In addition to these supplements and antibiotics, selective chocolate plates for the culture of GFP-*B. quintana* also contained 50 µg/mL kanamycin (Fluka Biochemika). Plates were poured, left to dry with lids agar for 15 minutes, stored inverted at 4°C, and used within one week.

2.2.3 LB broth

LB broth was made by adding 20 g of LB broth powder (Acumedia) to 1 L of water and autoclaving the solution.

2.2.4 *E. coli* culture

Liquid cultures of *E. coli* were made by adding a scrape of frozen culture or a colony from a plate into 5 mL of LB broth supplemented with ampicillin (Sigma-Aldrich) to a final concentration of 100 µg/mL. Liquid cultures were incubated overnight in a shaking incubator at 200 – 250 RPM and 37 °C.

For long-term storage, glycerol stocks of *E. coli* transformed with the MAL reporter plasmid were made by combining 500 µL of cryopreservation media (25% glycerol in water) and 500 µL of overnight growth liquid culture in a cryovial (Tarsons) and stored at -80 °C.

2.2.5 *Bartonella quintana* culture

Bartonella quintana were grown on chocolate agar plates in a humidified 37 °C incubator inside a glass jar with a lit candle to reduce O_2 and increase CO_2 levels. Plates were passaged every 5 – 7 days.

GFP-*B. quintana* were grown on selective chocolate plates supplemented with kanamycin, to maintain the GFP-pSRK plasmid, and with isopropyl β-D-1-thiogalactopyranoside (IPTG), to induce GFP expression. For each kanamycin selective chocolate plate, 40 µL of a 40 mg/mL stock of UltraPure™ IPTG (Invitrogen) was spread onto the plate and allowed to dry before adding GFP-*B. quintana* to the agar. GFP-*B. quintana* were incubated and passaged in the same way as wildtype *B. quintana*.

B. quintana cryopreservation media consisted of an autoclaved solution of 2.5% (w/v) Bacto™ heart infusion broth (BD) with 12.5% glycerol in water. *B. quintana* frozen stocks were made by scraping bacteria from chocolate plates into cryovials containing 0.5 – 1 mL of cryopreservation media and stored at -80 °C.

2.3 MAL reporter plasmid construction

Details of the MAL reporter plasmid and the empty vector used in its construction are listed in Table 2.2.

Table 2.2: Plasmids

Name	Description	Source
pcDNA3 mCherry LIC (6B)	Mammalian expression vector	Scott Gradia (Addgene plasmid #30125)
MAL reporter plasmid	MAL-mCherry fusion reporter plasmid for expression in mammalian cells	This study

2.3.1 MAL PCR amplification

A MAL DNA sequence was synthesized by Twist Bioscience and is shown in Appendix Figure 1. To clone the gene into a pcDNA3.1 vector a Kozak sequence was added to the 5′ end of the human MAL gene, as recommended by Thermo Fisher. This MAL DNA sequence was PCR amplified using the following primers (Integrated DNA Technologies), with the underlined bases corresponding to regions of overlap with the pcDNA3 mCherry LIC (6B) cloning vector.

MAL forward primer: 5′ - CGGATCCCTACTTCCAATCCAATATGCCACCGCTGAAGTCAC - 3′
MAL reverse primer: 5′ - CTGCCGTTGCTCCCACTACCAATTAGACAGCTGTCCCAATGGAG - 3′

A MAL PCR amplification reaction was set up as shown in Table 2.3 and run at the settings listed in Table 2.4.

Table 2.3: MAL PCR reaction

Reagent	Volume
Water	32.5 µL
5× Q5 Reaction Buffer (NEB)	10 µL
10 mM dNTPs (NEB)	1 µL
10 µM MAL forward primer (Integrated DNA Technologies)	2.5 µL
10 µM MAL reverse primer (Integrated DNA technologies)	2.5 µL
MAL template (Twist Biosciences)	1 µL
Q5 High-Fidelity DNA polymerase (NEB)	0.5 µL
Total volume	50 µL

Table 2.4: MAL PCR cycling settings

	Step	Temperature	Time
	Pre-cycle	98 °C	30 s
35 cycles	Denaturing	98 °C	10 s
	Annealing	55 °C	30 s
	Extension	72 °C	90 s
	Post-cycle	72 °C	2 min

The MAL PCR product was confirmed by gel electrophoresis and purified using a DNA Clean and Concentrator column (Zymo Research) according to the manufacturer's instructions.

2.3.2 Gibson assembly

The pcDNA3 mCherry LIC (6B) vector from Addgene was linearised by SspI (NEB) restriction digestion and purified with a DNA Clean and Concentrator column (Zymo Research). The linearised plasmid and the MAL PCR product were quantified using a NanoDrop ND-1000 Spectrophotometer (Thermo Fisher) to calculate the amounts required for Gibson assembly cloning[66].

To assemble the plasmid, 1.5 µL of MAL PCR product, 1 µL of linearised pcDNA3 mCherry LIC (6B) plasmid, 10 µL of 2× Gibson Assembly Mastermix (NEB), and 7.5 µL of water were combined and incubated at 50 °C for 15 minutes, then placed on ice.

2.3.3 Transformation

2.3.3.1 Preparing chemically competent cells

A liquid culture of One Shot™ TOP10 *E. coli* was set up and incubated overnight in a shaking incubator. The following morning, 1 mL of this overnight culture was added to 100 mL of LB broth and grown at 37 °C and 200 RPM until the culture reached an OD_{600} of 0.4 – 0.6. The culture was placed on ice for 10 minutes, divided into two pre-chilled 50 mL Falcon tubes, and pelleted by centrifugation at 2500 × *g* for 10 minutes at 4 °C. The supernatant was discarded, each cell pellet was resuspended in 50 mL of ice-cold 100 mM $MgCl_2$ (Sigma-Aldrich) and centrifuged as before. This step was repeated. Then, the supernatant was discarded and each cell pellet was resuspended in 2 mL of ice-cold 85 mM $CaCl_2$ (Sigma-Aldrich) in 15% glycerol. The cells were stored as 100 µL aliquots at -80 °C.

2.3.3.2 Transforming chemically competent cells

Following Gibson Assembly, 50 µL of chemically competent cells were thawed on ice for 10 minutes, 2 µL of the Gibson assembly reaction was added and the cells were incubated for 30 minutes on ice before being heat-shocked at 42 °C for 30 seconds, and then placed on ice. Transformed cells were rescued with LB broth, and 100 µL of various dilutions were spread onto LB agar plates supplemented with ampicillin. Plates were placed in a 5% CO_2 37 °C incubator overnight.

The next day, visible colonies were transferred to liquid cultures and incubated in a shaking incubator overnight.

2.3.4 Confirming plasmid construction

Plasmids were extracted from liquid cultures using the Monarch Plasmid Miniprep Kit (NEB) and digested with HindIII-HF and XbaI in rCutSmart™ Buffer (all NEB). An empty pcDNA3 mCherry LIC vector was included as a negative control. Gel electrophoresis was used to determine the size of digested plasmids.

Cultures whose plasmids had two fragments at 5 – 6 kbp (plasmid backbone) and 3 – 4 kbp (MAL-mCherry fusion) were used to make glycerol stocks which were stored at -80 °C. Plasmids from these cultures were quantified using a Qubit® 2.0 Fluorometer (Invitrogen), normalised to 300 ng in 10 – 15 of water, and sent to Plasmidsaurus for long-read sequencing using Oxford Nanopore Technologies. Sequencing results were analysed using Benchling software (2023)[67].

2.3.5 Preparing plasmid for transfection

Plasmid DNA for transfection was purified from 100 mL of overnight culture using NucleoBond® Xtra Midi kit (Macherey-Nagel) according to manufacturer instructions and eluted in 500 µL of TE buffer to achieve a final concentration of about 1 µg/µL. The concentrated purified plasmid was stored at -20 °C.

2.4 Mammalian cell culture

General cell culture media was RPMI 1640 with GlutaMAX™ and Phenol red (Gibco) supplemented with 10% heat-inactivated foetal calf serum (FCS) (Gibco) and Antibiotic-Antimycotic (Gibco). Unless specified otherwise, all cell culture reagents were warmed to 37 °C. Cells were incubated in 5% CO2 37°C incubators and counted using a haemocytometer (Hawksley).

2.4.1 HEK293T/17 cell culture

HEK293T/17 cells were kindly donated by Peter Pfeffer's lab and cultured in Nunc™ EasYFlask™ T-75 cell culture flasks (Thermo Fisher).

2.4.1.1 Thawing cells

A cryovial of cells was removed from liquid nitrogen and immediately thawed in a 37 °C water bath. The contents of the cryovial were then slowly added to 9 mL of media. Cells were spun at 300 × *g* for 4 minutes and resuspended in 5 mL of media. New T-75 tissue culture flasks were seeded by adding 5 mL of cell suspension to 20 mL of media. Cells were incubated until 70 – 90% confluent and then passaged.

2.4.1.2 Passaging cells

Once 70 – 90% confluent, flasks were removed from the incubator, media was poured off, cells were gently washed in 10 mL of PBS and incubated in 1 mL of 37°C Trypsin/EDTA solution (Gibco) for 2 – 5 minutes. The cells were then washed from the flask using 9 mL of media and centrifuged at 300 × *g* for 4 minutes. The pellet was resuspended in 10 mL of media and used to seed new flasks.

2.4.1.3 Freezing cells

Cells were pelleted at 300 × *g* for 4 minutes and resuspended in Recovery™ Cell Culture Freezing Medium (Gibco) to a final concentration of 1.5×10^6 cells/mL. Then, 1 mL aliquots were added to cryovials (Tarsons) which were slowly frozen in a CoolCell® LX (Biocision) at -80 °C for 24 hours before being transferred to liquid nitrogen for long-term storage.

2.4.1.4 HEK293T/17 transfection

After a minimum of three passages from frozen, cells were seeded onto surface-treated coverslips in 24-well plates (JET-BIOFIL) (see section 2.6.1) at a density 5×10^4 cells per well and incubated for at least 24 hours before the media was changed and cells were transfected. Transfections were performed using Lipofectamine™ 3000 Reagent (Invitrogen) or polyethyleneimine (PEI) (Fisher Scientific, catalog no. AA4389603) at a concentration of 1 mg/mL in PBS.

Lipofectamine transfections were carried out as follows, quantities correspond to one well in a 24-well plate and were scaled up accordingly. DNA-Lipofectamine complexes were prepared by combining 0.75 µL of Lipofectamine™ 3000 Reagent and 25 µL of Opti-MEM™ Reduced Serum Medium (Gibco) in one tube, adding 1 µL of P3000™ Reagent and

0.5 µg of DNA to 25 µL of Opti-MEM™ Reduced Serum Medium in another tube, and then combining 25 µL from each tube and gently mixing by flicking. After 10 – 15 minutes of incubation at room temperature, 50 µL of this DNA-lipid complex was slowly dripped onto the cells.

PEI transfections were carried out as follows. For each well in a 24-well plate, 1 µg of DNA was added to 3 µL of room temperature PEI and incubated at room temperature for 5 – 10 minutes. The transfection mix was then diluted in media at a 1:5 ratio and 20 µL of the final solution was added to each well.

All transfected cells were incubated for 24 hours before serum starvation.

2.4.2 THP-1 cell culture

THP-1 cells were grown in Greiner Bio-One CELLSTAR® 50 mL suspension cell culture flasks. For differentiation and *B. quintana* infection experiments, THP-1 cells were grown on surface-treated coverslips in 24-well plates (see section 2.6.1).

2.4.2.1 Thawing cells

Recovery media for thawing THP-1 cells was general cell culture media supplemented with 20% FCS instead of 10% FCS. Cryovials were thawed in a 37 °C water bath and the contents were slowly added to 4 mL of recovery media. A 10 µL sample of the cell suspension was counted to calculate cell concentration. Cells were spun at 200 × *g* for 5 minutes, resuspended in 5 mL of recovery media, spun at 200 × *g* for 5 minutes, resuspended to a final concentration of 5×10^5 cells/mL, and transferred to suspension flasks. Cells were incubated in flasks upright for 5 – 7 days. Every 2 – 3 days, cells were removed from the flask, spun down as before, resuspended in the same volume of recovery media, and transferred into a fresh flask. Once cells reached a concentration of $1 – 1.5 \times 10^6$ cells/mL, they were passaged.

2.4.2.2 Passaging cells

THP-1 cells were washed from suspension flasks with general media, transferred to a 50 mL Falcon tube and spun at 200 × *g* for 5 minutes. Cells were then resuspended in general media to a final concentration of 5.5×10^5 cells/mL and transferred into new suspension flasks, which were incubated horizontally.

2.4.2.3 PMA differentiation

THP-1 cells were differentiated into macrophage-like cells using phorbol 12-myristate-13-acetate (PMA) (AG Scientific). Differentiation media consisted of general cell culture media

supplemented with 10 ng/mL of PMA. Cells were seeded onto coverslips in 24-well plates in differentiation media at a concentration of 2×10^5 cells per well. After 48 hours of incubation, cells were serum starved.

2.5 Infection and stimulation of mammalian cells

2.5.1 Serum starvation

All serum starvation media was antibiotic-free. The different types of media used included: RPMI 1640 with 0.3% FCS; serum-free DMEM with GlutaMAX™, high glucose and Phenol red (Gibco); and serum-free RPMI 1640. Cells were serum starved for 20 – 24 hours before experiments.

2.5.2 Infection with *B. quintana*

A stock solution of *B. quintana* in serum starvation media was made using bacteria scraped from confluent 5-day-old chocolate plates. A NanoDrop ND-1000 Spectrophotometer (Thermo Fisher) was used to measure the OD_{600} of the bacterial cell suspension, which was used to estimate the amount of *B. quintana* present, assuming an OD_{600} value of 1 corresponded to 1×10^9 cells/mL. The stock solution of *B. quintana* was diluted as required and used to infect cells. For each well in a 24-well plate, 100 µL of *B. quintana* suspension was added to the existing 900 µL of serum starvation media, giving a final volume of 1 mL per well. Infected cells were incubated for 1.5 hours at 37 °C and 5% CO_2. To confirm the number of live bacteria present, serial dilutions of the *B. quintana* stock solution were plated on chocolate plates and incubated for 10 days until visible colonies formed.

Infection with GFP-*B. quintana* was performed in the same way, but with serum starvation media supplemented with 1 mM IPTG, giving a final concentration of 0.1 mM IPTG in each well.

2.5.3 LPS stimulation

After 1.5 hours of infection with *B. quintana*, THP-1 cells were stimulated with 100 ng/mL of lipopolysaccharide (LPS) from *E. coli* O111:B4 (Sigma-Aldrich) for 0 – 3 hours at 37 °C and 5% CO_2. LPS stimulation media was serum starvation media supplemented with 0.1 mM IPTG and 200 ng/mL LPS. For each well in a 24-well plate, 1 mL of LPS media was added to the existing 1 mL of infection media, giving a final concentration of 100 ng/mL LPS and 0.1 mM IPTG in each well.

2.6 Microscopy

The antibodies and stains used for microscopy are listed in Table 2.5.

Table 2.5: Antibodies and stains

Antibodies	Use	Target	Host species	Species reactivity	Excitation/ Emission wavelength	Source
MKL1 polyclonal antibody	Primary antibody to detect endogenous MAL	MKL1/ MAL	Rabbit	Human	N/A	Invitrogen (PA5-56557)
Polyclonal secondary antibody with Alexa Fluor™ 568	Secondary antibody conjugated to a fluorophore	IgG	Goat	Rabbit	579/603 nm (orange-red)	Invitrogen (A-11011)
Stains	**Use**	**Target**		**Excitation/Emission wavelength**		**Source**
DAPI (4′, 6-diamidino-2-phenylindole, dihydrochloride)	DNA stain to visualise cell nuclei and bacteria	DNA		360/460 nm (blue)		Thermo Fisher
Fluorescein phalloidin	Actin stain to visualise cells	F-actin		496/516 nm (green)		Thermo Fisher
Alexa Fluor™ 647 phalloidin	Actin stain to visualise cells	F-actin		650/688 nm (far-red)		Thermo Fisher

2.6.1 Surface-treated coverslips

Round 13 mm coverslips (Marienfeld) were autoclaved, placed into 24-well plates (JET-BIOFIL), treated with 0.1 mg/mL Poly-D-lysine (Gibco) for 1 hour at room temperature, rinsed three times with water, and allowed to dry. Surface-treated coverslips in plates were either used immediately or sealed tightly with parafilm and stored at 4 °C for up to one week.

2.6.2 Fixing and permeabilising cells

Cells were fixed by incubation in complete paraformaldehyde fixation solution (see section 2.1.2) for 30 minutes at room temperature, followed by three washes with PBS. Cells were permeabilised for 15 minutes with 0.1% (v/v) Triton-X-100 (Sigma) in PBS and washed three times in PBS. HEK293T/17 cells (which were transfected with a MAL reporter plasmid)

were then stained for actin and DNA, whilst THP-1 cells were blocked and stained with antibodies against MAL.

2.6.3 Blocking and antibody staining

Blocking buffer consisted of 1% Blocker™ BSA (Thermo Fisher) in PBS. For 24-well plates, 300 µL of blocking buffer was added to each well. THP-1 cells were blocked for 1 hour at room temperature. Cells were then incubated with MKL1 polyclonal antibody diluted 1:1000 in blocking buffer (200 µL per well) in the dark at 4 °C overnight with no agitation. The following morning, cells were washed three times in PBS and incubated with secondary antibody diluted 1:1000 in blocking buffer (200 µL per well) for 1 hour in the dark at room temperature. Cells were then washed three times in PBS and stained for actin and DNA.

2.6.4 Actin and nuclear staining

Cells infected with wildtype *B. quintana* were stained for actin using a FITC-phalloidin stain diluted 1:400 in PBS. Cells infected with GFP-*B. quintana* were stained for actin using an Alexa Fluor™ 647-phalloidin stain diluted 1:400 in PBS. In both cases, 200 µL of actin stain was added to each well of a 24-well plate, cells were incubated for 30 minutes in the dark, and then washed three times in PBS. To stain cell nuclei, cells were incubated for 5 minutes in the dark with a 1 µg/mL DAPI (Thermo Fisher) solution in PBS. Cells were then washed three times in PBS and coverslips were mounted onto slides using ProLong™ Diamond Antifade Mounting Medium (Invitrogen). Slides were cured at room temperature in the dark for 24 hours, sealed with clear nail polish, and stored in the dark at -20 °C.

2.6.5 Image acquisition and analysis

Slides were imaged using an IN Cell Analyzer 6500 high throughput microscope (Cytiva) or an Olympus BX61 Fluorescence microscope, and images were analysed using FIJI software [65]. Each sample was performed with three biological replicates, and three technical replicates were generated from each biological replicate. For each technical replicate, an average of 50-100 cells were manually labelled as having nuclear, cellular, or cytoplasmic MAL-mCherry.

2.6.6 Statistical analyses

For experiments with one dependent variable, the differences between conditions were analysed using one-way ANOVA tests with Tukey's multiple comparison tests assuming equal SDs. Differences between conditions across a set of three independent experiments were analysed using two-way ANOVA tests with Tukey's multiple comparison tests (to

compare different conditions within one experiment and to compare the same condition across different experiments). For experiments investigating the effects of LPS and multiplicity of infection (MOI), the differences between conditions were analysed using two-way ANOVA tests with Tukey's multiple comparisons tests (to compare different timepoints of LPS stimulation with the same MOI) and Sidak's multiple comparisons tests (to compare different MOIs with the same timepoint of LPS stimulation). The normality of each data set was visually analysed using residual and QQ plots.

Chapter 3 - Investigating the effects of *B. quintana* on MAL in HEK293T/17 cells

3.1 Introduction

MAL is a central signalling molecule in several cellular processes, including actin dynamics, changes in cell morphology, and migration[46]. There is evidence that *B. quintana* targets these processes, but some of its specific effects on host cell signalling, including its effect on MAL, have not been characterised[23,29]. Determining whether *B. quintana* affects MAL or not could contribute to better understanding of the molecular interactions between Type-IV-secreted proteins, or Beps, and host cell signalling and help identify the specific downstream cellular processes that are disrupted by *B. quintana*.

As a transcriptional cofactor, MAL's effects on cellular processes are mainly driven by changes in gene expression, which require the accumulation of MAL in the nucleus[41]. In resting cells, MAL shuttles continuously between the nucleus and cytoplasm which leads to cellular distribution of MAL[40]. When MAL is activated, its nuclear export is blocked, causing it to accumulate in the nucleus[40]. Nuclear accumulation of MAL correlates with increased activation of the MAL/SRF pathway[40,41]. Thus, the subcellular localisation of MAL can be used as a proxy for MAL/SRF activation. For example, the effects of *Enteropathogenic E. coli* (EPEC) on the host MAL/SRF pathway were investigated using fluorescence microscopy to measure the nuclear accumulation of MAL-GFP in mammalian cells in response to bacteria[64].

We therefore sought to establish a tissue culture model that would measure the subcellular localisation of MAL in response to *B. quintana*, as a way of determining whether *B. quintana* activates MAL. This model involved constructing a MAL reporter plasmid and transfecting it into HEK293T/17 cells, causing them to express a fluorescent MAL-mCherry fusion protein. The subcellular localisation of MAL-mCherry was then visualised using fluorescence microscopy, allowing the effect of *B. quintana* on MAL's distribution to be explored. We reasoned that using a high-copy MAL reporter plasmid, rather than directly staining endogenous MAL with antibodies, would amplify the fluorescent signal resulting from changes in MAL's subcellular localisation, making it easier to visualise and quantify. Additionally, since HEK293T/17 cells are easy to maintain and large quantities of MAL

reporter plasmid can be readily made, this model has the potential to be easily upscaled to investigate a range of different conditions.

This chapter describes the construction and validation of the MAL reporter plasmid, its transfection into mammalian cells, and the subcellular localisation of MAL in transfected cells in response to *B. quintana* infection.

3.2 Results

3.2.1 MAL reporter plasmid construction

A MAL reporter plasmid was constructed using the mammalian expression vector pcDNA3 mCherry LIC (6B) from Addgene[68]. This plasmid adds mCherry to the C-terminus of MAL, thus creating a MAL-mCherry fusion gene. The vector contains a CMV promoter and enhancer, to drive constitutive expression of the MAL-mCherry fusion gene in mammalian cells; an ampicillin resistance gene, allowing bacteria transformed with the plasmid to be selected for using ampicillin-supplemented media; and an origin of replication which allows the plasmid to replicate and be maintained in *E. coli*.

A MAL DNA sequence synthesized by Twist Biosciences was amplified by PCR with primers designed to add ligation independent cloning sequences to the ends of the MAL gene (see section 2.3.1). The resulting PCR product was run on a 1% agarose gel and scanned, as shown in Figure 3.1.

.

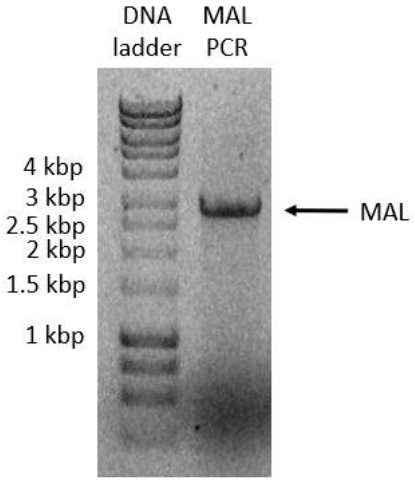

Figure 3.1: Gel electrophoresis of MAL PCR product. The right lane of the gel shows a strong band at 3 kbp, which corresponds to the expected size of the MAL PCR product.

Since the MAL gene is 2.83 kbp and the gel shown in Figure 3.1 shows a strong band at 3 kbp, this suggested that MAL was correctly amplified, so I proceeded with cloning. In preparation for Gibson assembly, the empty pcDNA3 mCherry LIC vector was linearised by

SspI digestion, as recommended by Addgene[68]. The MAL PCR product and linearised vector were purified and quantified separately, then assembled using Gibson assembly. The assembled plasmids were transformed into chemically competent *E. coli* which were grown overnight on selective plates. The following morning, visible colonies were used to inoculate liquid cultures which were grown overnight. Plasmids were extracted from these liquid cultures and used to test whether plasmids had been correctly assembled.

3.2.2 Validation of plasmid construction

To test whether plasmids had incorporated the MAL PCR product, a XbaI HindIII-HF double digest was used, as recommended by Addgene[68]. Within the pcDNA3 mCherry LIC (6B) plasmid, XbaI and HindIII-HF are enzymes with unique restriction sites either side of the insert, so performing a double digest with these enzymes will result in two fragments, one corresponding to the plasmid backbone, and one corresponding to the insert. If cloning is successful, the insert will contain the MAL gene and mCherry, but if cloning is unsuccessful, the insert will only contain mCherry. The results of this digest are shown in Figure 3.2.

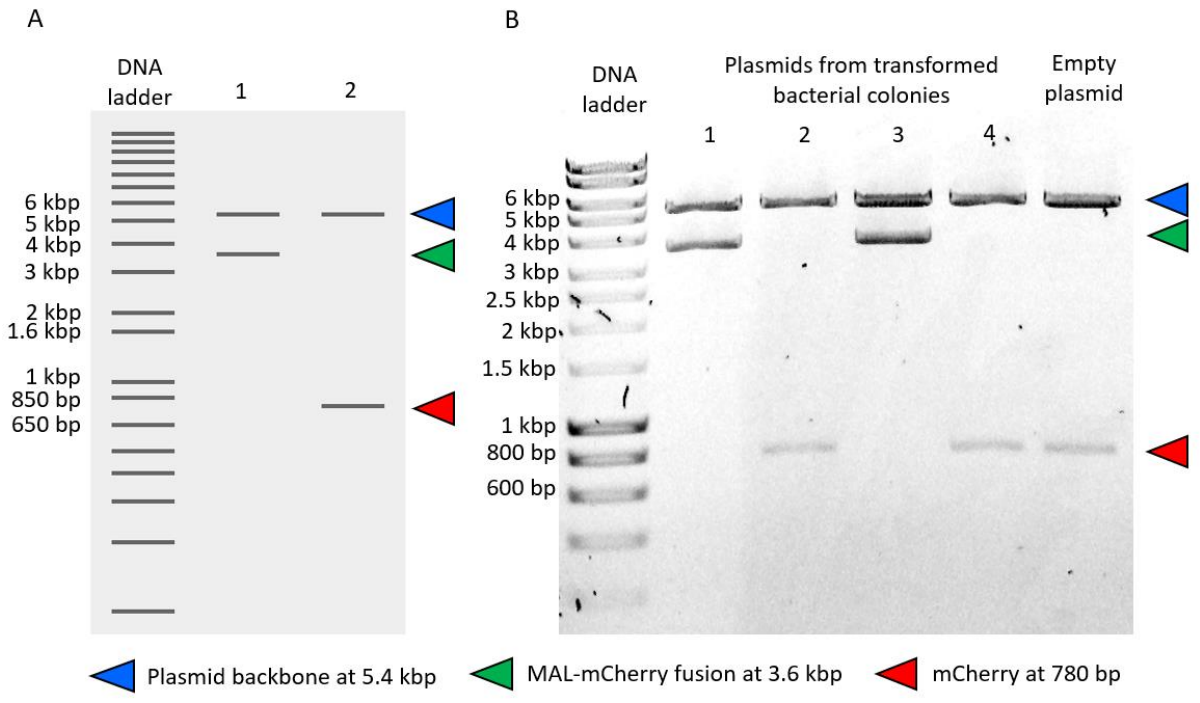

Figure 3.2: XbaI HindIII-HF double digest of MAL reporter plasmid. A: Virtual XbaI HindIII-HF double digest of plasmid with MAL (lane 1) and empty plasmid (lane 2)[67]. B: Gel electrophoresis of XbaI HindIII-HF double digest of plasmids extracted from transformed *E. coli* (lanes 1-4) and empty plasmid. Lanes 2 and 4 have bands at 5-6 kbp and 800 bp, which match the bands from the empty plasmid. Lanes 1 and 3 match lane 2 of Figure 3.2A and have bands at 5-6 kbp and 3-4 kbp. This latter fragment corresponds to the MAL-mCherry fusion gene.

Figure 3.2 shows the results of a virtual digest created using Benchling software and the double digest of plasmids extracted from transformed bacterial colonies[67]. Liquid cultures with plasmids containing MAL, such as the ones seen in lane 1 and 3 of Figure 3.2B, were used to make glycerol stocks for long-term storage. Plasmids from these cultures were sent to Plasmidsaurus for sequencing, to confirm that MAL and mCherry were in the same reading frame and would therefore be expressed as a single fusion gene.

3.2.3 MAL-mCherry subcellular localisation in mammalian cells

Once the MAL reporter plasmid had been constructed and validated, it was used to transfect HEK293T/17 cells. Briefly, HEK293T/17 cells were grown on glass coverslips, incubated for 24 hours, and transfected with the MAL reporter plasmid. Cells were fixed 48 hours after transfection, stained for actin and DAPI, and mounted onto slides. Some representative images of MAL-mCherry in transfected cells are shown in Figure 3.3.

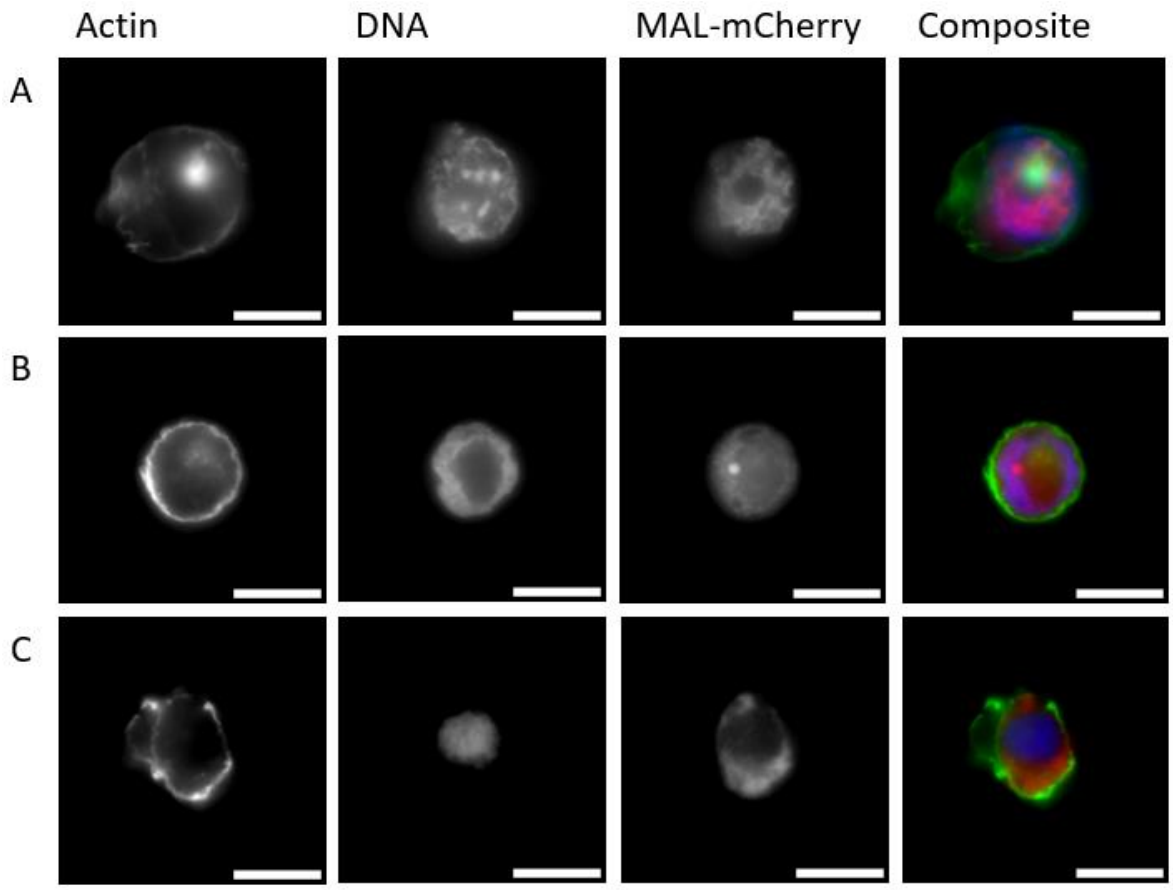

Figure 3.3: MAL-mCherry subcellular localisation. Microscopy images showing the subcellular localisation of MAL-mCherry in transfected HEK293T/17 cells. Images were taken at 100× magnification and scale bars represent 10 µm. From left to right, images show F-actin stained with FITC-phalloidin, DNA stained with DAPI, MAL-mCherry, and composite images with actin in green, DNA in blue, and MAL-mCherry in red. A, B, and C show cells with nuclear, cellular, and cytoplasmic MAL-mCherry, respectively.

Three main types of MAL-mCherry fluorescence were observed in transfected cells, as shown in Figure 3.3. In Figure 3.3A, MAL is restricted to the nucleus; in Figure 3.3B, MAL is found in the nucleus but also in the rest of the cell; and in Figure 3.3C, MAL is excluded from the nucleus. These three phenotypes correspond to nuclear, cellular, and cytoplasmic MAL distribution, respectively. In subsequent experiments, the relative abundance of each of these three types of MAL distribution were counted, and the percent of cells with nuclear MAL was used as a proxy for MAL/SRF activation. A typical field of view (FOV) is shown in Figure 3.4.

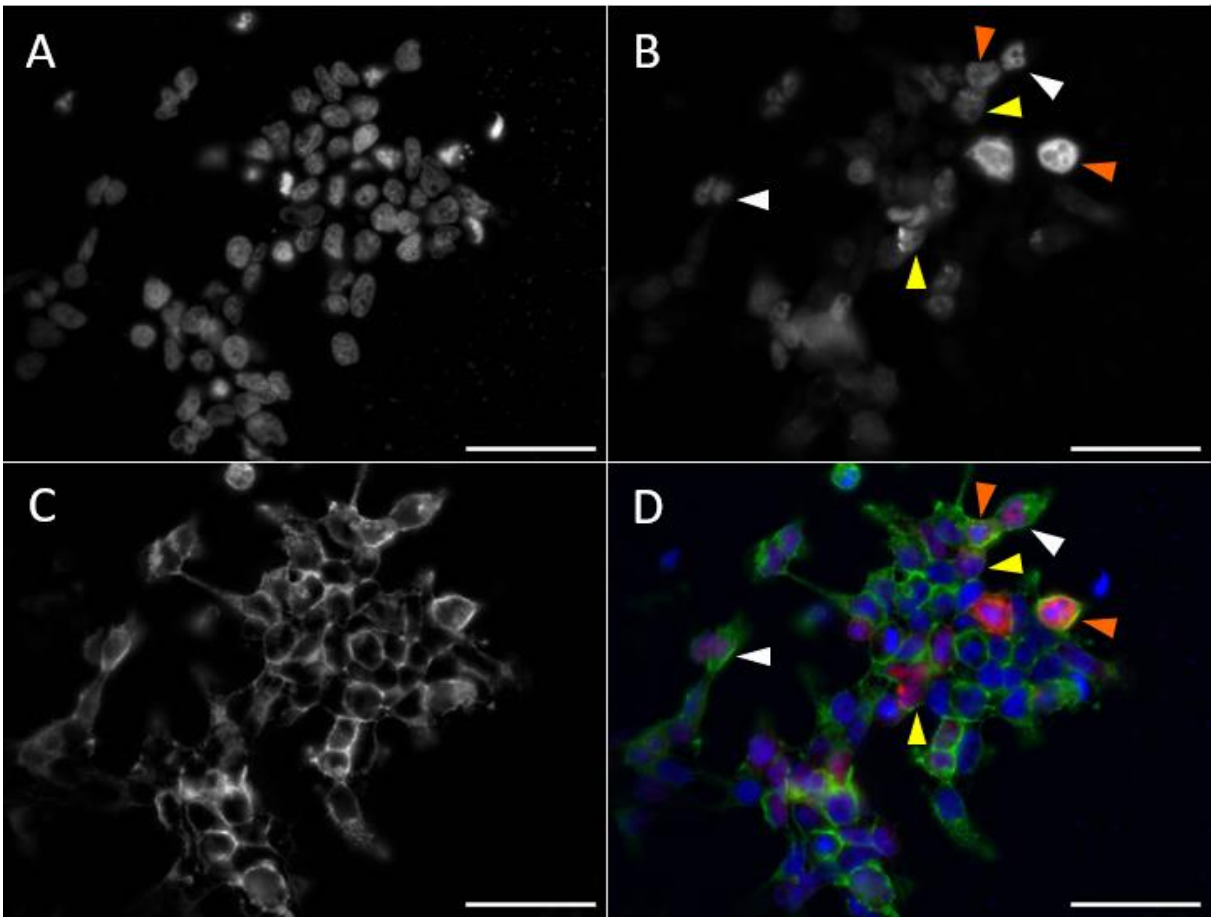

Figure 3.4: Representative FOV of transfected HEK293T/17 cells. Microscopy images showing transfected, serum-starved, uninfected HEK293T/17 cells. Images were taken at 60× magnification and scale bars correspond to 50 µm. A: DNA stained with DAPI. B: MAL-mCherry. C: F-actin stained with FITC-phalloidin. D: Composite image showing DNA in blue, MAL-mCherry in red, and actin in green. Different phenotypes of MAL-mCherry distribution are shown on B and D, with white, yellow, and orange arrows representing nuclear, cellular, and cytoplasmic MAL, respectively.

I aimed to use imaging software to automatically determine the percent of cells with nuclear MAL-mCherry, by defining cells as nuclear if they had greater mCherry fluorescence in the nucleus than the cytoplasm. However, the available software was unable to accurately detect cell borders, and thus unable to define nuclear and cytoplasmic regions within cells. This is

likely due to the variable morphology of HEK293T/17 cells and their tendency to form dense clumps of cells, as shown in Figure 3.4. Therefore, manual cell counting was used to determine the percent of cells with nuclear MAL-mCherry in each condition.

3.2.4 Serum stimulation of transfected HEK293T/17 cells

Serum is a potent activator of the MAL/SRF pathway and induces rapid nuclear accumulation of MAL[40,41,44]. A previous study of MAL in HEK293 cells found that stimulation with 15% FCS increases the percent of cells with nuclear MAL from 10% (0 minutes of stimulation) to 80% in 5 minutes[69]. Nuclear accumulation of MAL then decreases after this peak and by 60 minutes of serum stimulation, 40-50% of cells have nuclear MAL[69]. Based on these methods, I aimed to use serum stimulation as a positive control for MAL-mCherry nuclear localisation. Briefly, transfected HEK293T/17 cells were serum starved for 24 hours, stimulated with media containing 15% FCS, fixed at different timepoints of serum stimulation, stained, and imaged. The results of these experiments are shown in Figure 3.5.

Serum stimulation with 15% FCS did affect MAL-mCherry nuclear localisation ($p=0.0114$), but not in the way I expected, based on previous studies[64,69]. The percent of cells with nuclear MAL-mCherry in the negative control (0 minutes of serum stimulation) is higher than expected. I expected to see a peak in nuclear MAL-mCherry levels at 2-10 minutes, but at these timepoints MAL-mCherry nuclear accumulation did not increase compared to the negative control. There was significantly less MAL-mCherry nuclear localisation at 60 minutes of FCS stimulation than at 0 minutes ($p=0.0204$). There were also significant differences between experimental replicates ($p=0.0006$). The data shown in Figure 3.5 vary between experiments, are not supported by previous studies, and therefore cannot be used as a positive control for MAL-mCherry nuclear localisation[69]. Due to time constraints, this was not further investigated and a positive control for MAL nuclear accumulation and MAL/SRF activation was not included in subsequent experiments.

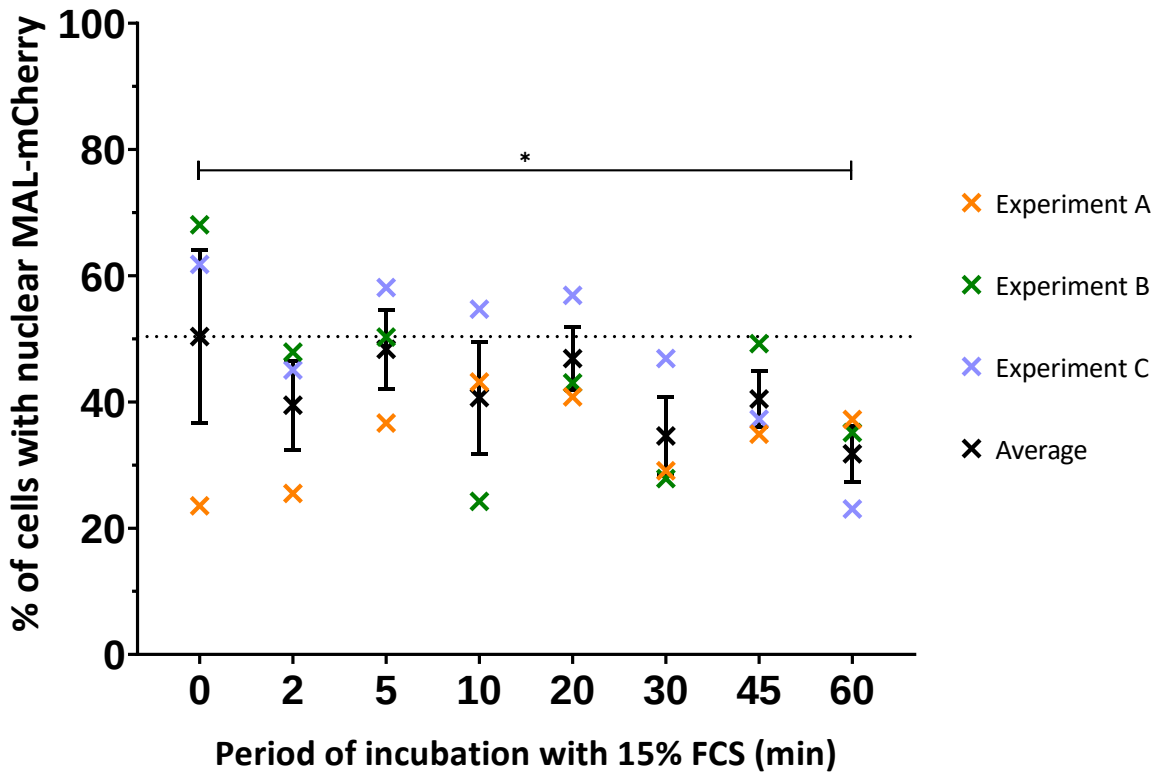

Figure 3.5: MAL-mCherry nuclear localisation in HEK293T/17 cells in response to serum stimulation. Each data point represents the mean percent of cells with nuclear MAL-mCherry in each condition of each experiment, across three biological replicates. Different colours correspond to different experiments, whilst black represents the mean across all experiments, with error bars showing SEM. The dotted line represents the mean percent of cells with nuclear MAL-mCherry in the negative control (0 min). *p<0.05. Two-way ANOVA with Tukey's multiple comparisons tests. Non-significant differences are not shown.

3.2.5 Infection of transfected HEK293T/17 cells with *B. quintana*

To determine the effect of *B. quintana* on the MAL/SRF pathway, the distribution of MAL in infected and uninfected cells was compared using the techniques described above. Briefly, HEK293T/17 cells transfected with the MAL reporter plasmid were serum starved for 24 hours and then infected with *B. quintana* for 90 minutes, at multiplicities of infection (MOIs) ranging from 0 to 1000. Multiple MOIs were used to determine whether the effect of *B. quintana* on MAL's subcellular localisation was dose dependent. Following infection, cells were fixed, stained, mounted onto slides, and imaged. The generated images were used to determine the mean percent of cells with nuclear MAL-mCherry in each condition.

The results of three independent infection experiments are shown in Figure 3.6. As shown in Figure 3.6A, cells infected with *B. quintana* at a MOI of 500 and 1000 had significantly increased MAL-mCherry nuclear localisation compared to uninfected cells (p=0.0133 and p=0.0333, respectively). Across experiments B and C, there were no significant differences in MAL-mCherry nuclear localisation in cells infected with different MOIs. The increase in MAL-mCherry nuclear localisation seen in experiment A was not reproduced in the two latter experiments, therefore it is unlikely to show the effects of *B. quintana* infection. To determine if there were any consistent differences in MAL-mCherry nuclear localisation resulting from *B. quintana* infection, the data from the three experiments shown in Figure 3.6 were graphed together. The results are shown in Figure 3.7.

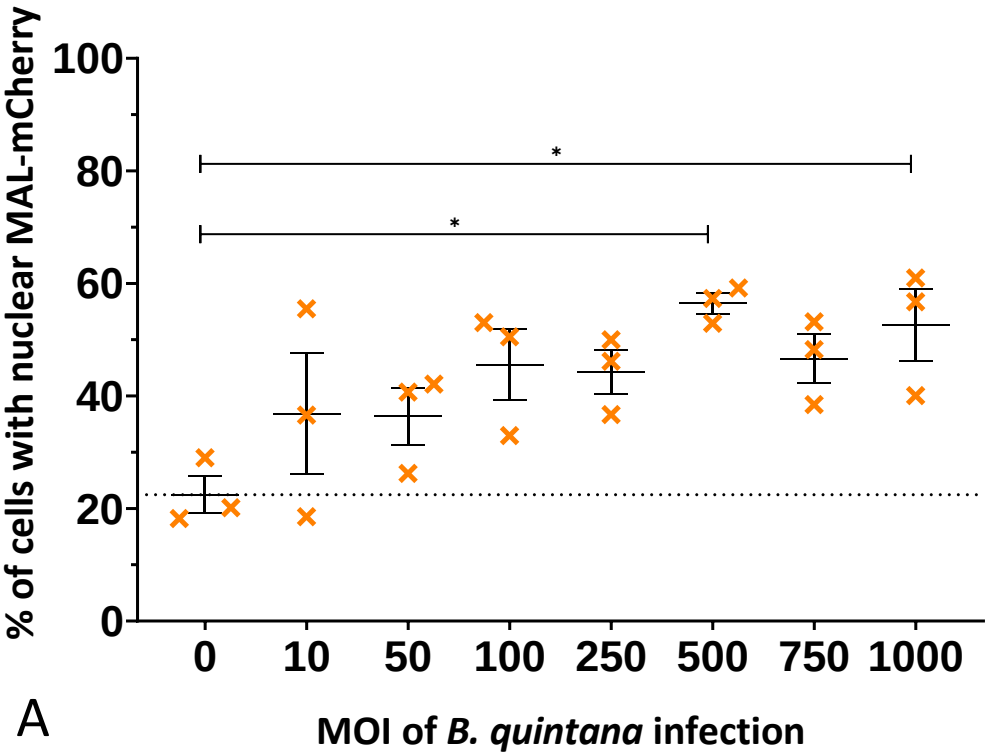

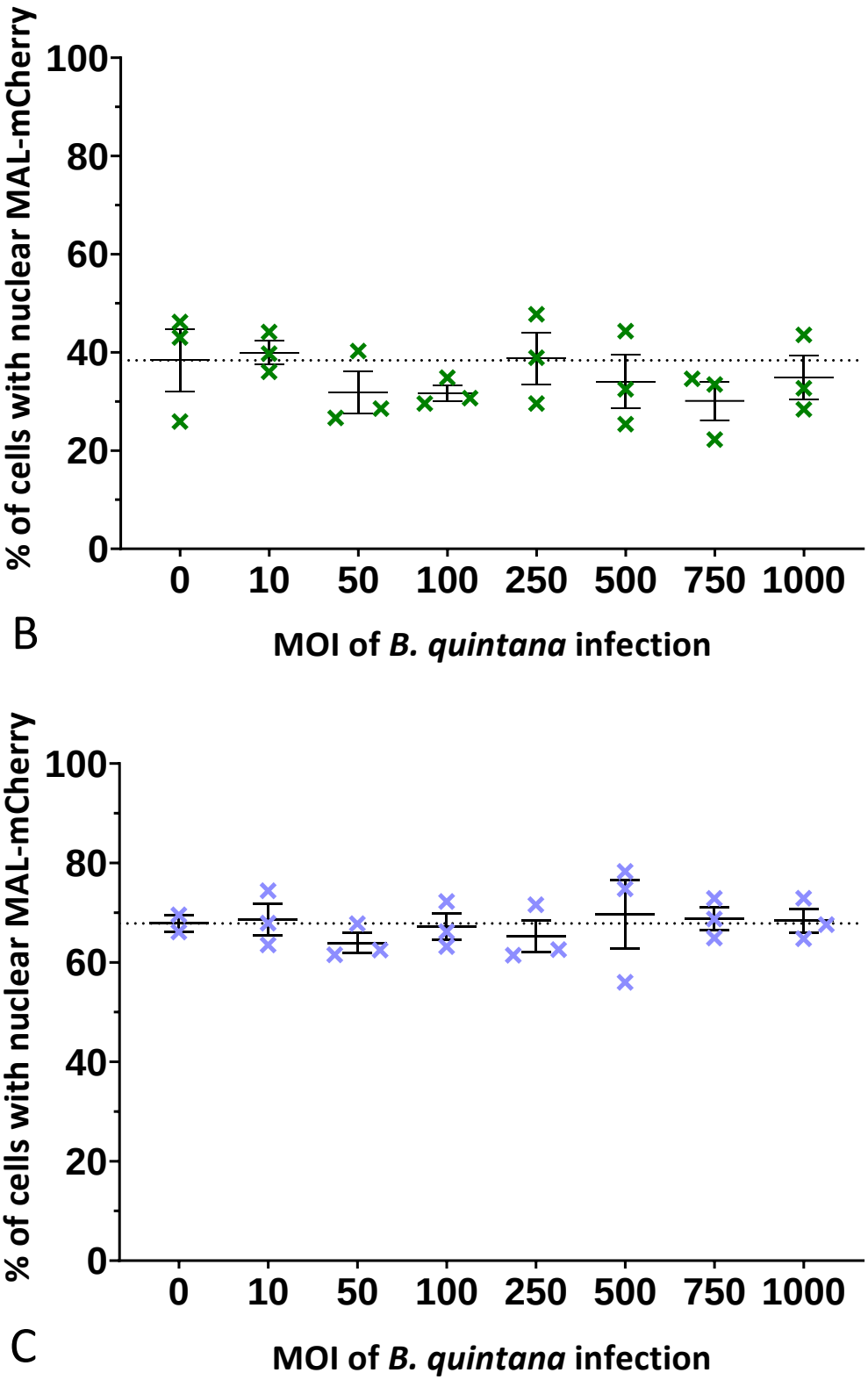

Figure 3.6: MAL-mCherry nuclear localisation in transfected HEK293T/17 cells in response to *B. quintana.* A, B, and C show three independent experiments. Each data point corresponds to one biological replicate. Error bars represent the mean and SEM across three biological replicates. Dotted lines represent the mean percent of cells with nuclear MAL-mCherry in the negative control (MOI 0) for each experiment. *p<0.05. One-way ANOVA with Tukey's multiple comparisons tests. Non-significant differences are not shown.

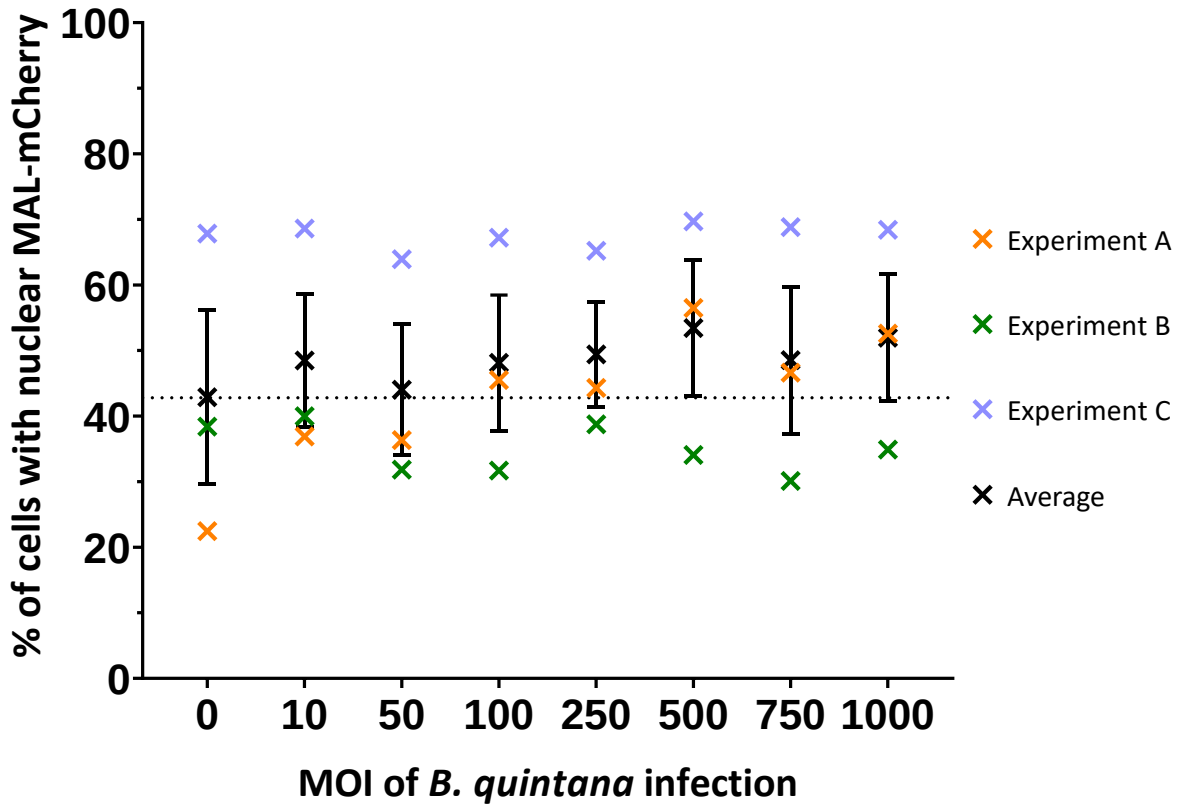

Figure 3.7: The effects of *B. quintana* and experiment on MAL-mCherry nuclear localisation in HEK293T/17 cells. Each data point represents the mean percent of cells with nuclear MAL-mCherry in each condition of each experiment, across three biological replicates. Different colours correspond to different experiments, whilst black represents the mean across all experiments, with error bars showing SEM. The dotted line represents the mean percent of cells with nuclear MAL-mCherry in the negative control (MOI 0). Two-way ANOVA with Tukey's multiple comparisons tests. Non-significant differences between different MOIs ($p \geq 0.05$) are not shown.

Comparing the average nuclear localisation of MAL-mCherry for different MOIs across all experiments, shown in black on Figure 3.7, did not show any significant differences ($p=0.1508$). However, there was a significant difference in nuclear localisation of MAL-mCherry between experiments ($p<0.0001$).

Overall, the results of Figure 3.6 and Figure 3.7 and do not conclusively show whether *B. quintana* affects MAL-mCherry nuclear localisation in transfected HEK293T/17 cells or not. There are significant differences in the same condition of different experiments, which is unexpected. In particular, the percent of cells with nuclear MAL-mCherry in the negative control (MOI 0) varies between experiments. The cells in these conditions are serum-starved and are therefore expected to have consistently low levels of nuclear MAL-mCherry, based on previous studies[64,69]. Since this was not seen in experiments shown in Figure 3.7, and the

effect of *B. quintana* on MAL cannot be assessed without a reliable negative control, the subcellular distribution of MAL-mCherry in serum-starved cells was further investigated.

3.2.6 Investigating the effects of serum starvation on transfected HEK293T/17 cells

Serum starvation is an established negative control for MAL nuclear accumulation, with 20 – 24 hours of incubation in both serum-free media and media supplemented with 0.3% FCS resulting in about 10% of treated cells with nuclear MAL[64,69]. However, the percent of cells with nuclear MAL-mCherry in serum-starved cells in the experiments shown in Figure 3.7 varied between about 20% and 70%. Therefore, the subcellular localisation of MAL-mCherry in serum starved cells was further investigated. Two different methods of serum starvation were tested: RPMI media supplemented with 0.3% FCS and serum-free DMEM. The results are shown in Figure 3.8.

The percent of cells with nuclear MAL-mCherry in cells serum starved with RPMI supplemented with 0.3% FCS (shown in Figure 3.8A) differed significantly across experiments. Experiment 1 had significantly lower levels of nuclear MAL-mCherry than experiments 2, 3, 4, and 5 ($p<0.0001$, $p=0.0002$, $p<0.0001$, and $p=0.0068$, respectively). Experiment 2 had significantly higher levels of nuclear MAL-mCherry than experiments 3 and 5 ($p=0.0497$ and $p=0.0008$, respectively). Experiment 4 had significantly higher levels of nuclear MAL-mCherry than experiment 5 ($p=0.0058$). Similarly, levels of nuclear MAL-mCherry in cells serum starved in serum-free DMEM (shown in Figure 3.8B) differed significantly across experiments. Experiment 2 had lower levels of nuclear MAL-mCherry than experiments 1 and 3 ($p=0.0306$ and $p=0.0162$, respectively). Overall, Figure 3.8 shows that there are significant differences in MAL-mCherry subcellular localisation at 20 – 24 hours of serum starvation, which is unexpected. All of the biological replicates for serum-starved (or MOI 0) cells shown in Figure 3.6 and in Figure 3.8 have more than 10% of cells with nuclear MAL-mCherry, which is the expected baseline for serum-starved cells, based on previous studies[64,69].

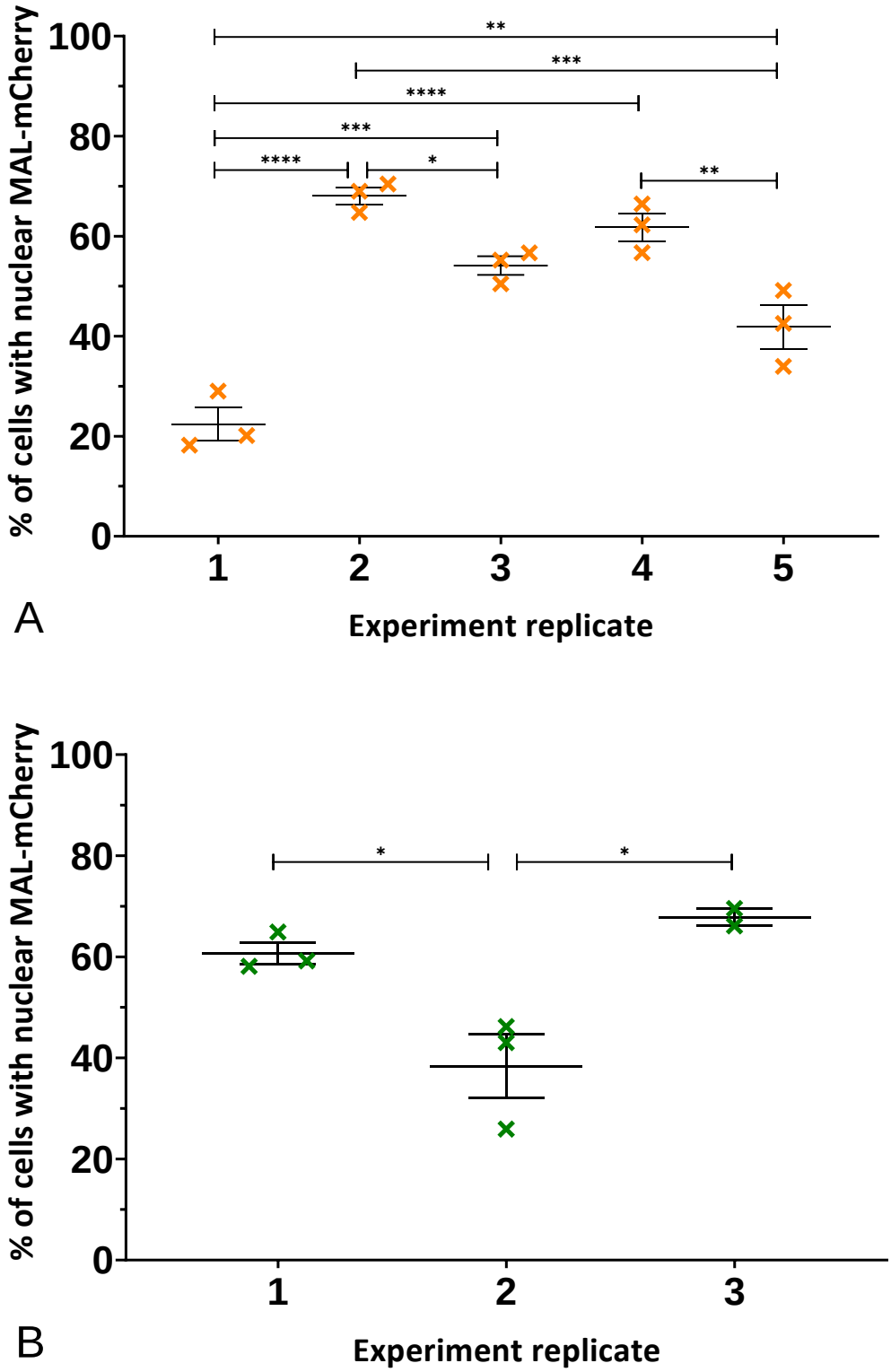

Figure 3.8: MAL-mCherry nuclear localisation in serum-starved HEK293T/17 cells. A: MAL-mCherry localisation in response to RPMI supplemented with 0.3% FCS across five experiments. B: MAL-mCherry localisation in response to serum-free DMEM across three experiments. Each data point corresponds to one biological replicate. Error bars represent the mean and SEM across three biological replicates. *p<0.05; **p<0.01; ***p<0.001; ****p<0.0001. One-way ANOVA with Tukey's multiple comparisons tests. Non-significant differences are not shown.

3.3 Discussion

The aim of the experiments described in this chapter was to develop a model to assess the effects of *B. quintana* on MAL nuclear localisation in mammalian cells. Since MAL nuclear accumulation is a proxy for MAL/SRF activation, this enables the effects of *B. quintana* on the MAL/SRF pathway to be investigated. A MAL-mCherry reporter plasmid was constructed and transfected into HEK293T/17 cells, allowing the subcellular localisation of MAL-mCherry to be visualised by fluorescence microscopy. Transfected cells were then infected with *B. quintana* and the changes in MAL nuclear accumulation were measured to determine whether *B. quintana* activates MAL.

Whilst the three main phenotypes of MAL-mCherry subcellular distribution (nuclear, cellular, and cytoplasmic distribution, shown in Figure 3.3A, B, and C, respectively) observed matched those seen in similar studies, I did not observe an increase in MAL-mCherry nuclear accumulation in response to serum stimulation, which was unexpected[64,69]. In infection experiments, MAL's subcellular localisation was found to differ significantly within each condition tested. Therefore, the changes in MAL's nuclear accumulation shown in Figure 3.6 and Figure 3.7 cannot be conclusively attributed to *B. quintana*.

The data shown in Figure 3.6A suggested that *B. quintana* caused an increase in nuclear MAL-mCherry at MOIs of 500 and 1000, but this result could not be replicated in further experiments. Moreover, the subcellular localisation of MAL-mCherry was found to be highly variable between experiments run at different times, but did not vary between different MOIs of *B. quintana* infection, as shown in Figure 3.7. Upon further investigation, MAL-mCherry subcellular localisation was found to differ significantly in uninfected serum-starved cells, as shown in Figure 3.8. These results show that the percent of serum-starved cells with nuclear MAL is well above the expected baseline level of 10%, and the same pattern was seen using two different established methods of serum starvation, so there must be some other unknown factor affecting the subcellular localisation of MAL[64,69].

Transfection involves introducing double-stranded DNA into a eukaryotic cell, and previous work in the lab found that transfecting HeLa cells with an empty plasmid is enough to activate some innate immune responses[70]. The purpose of transfection in the experiments described above was to allow MAL to be visualised, so transfecting HEK293T/17 cells with an empty plasmid would have required antibody staining to detect and analyse the subcellular distribution of MAL. It would be worthwhile to use antibody staining to compare the nuclear

accumulation of endogenous MAL in untransfected HEK293T/17 cells and cells transfected with an empty plasmid, to determine if transfection does significantly affect MAL. However, this would not explain the differences in MAL nuclear localisation seen in Figure 3.6, since all these cells were transfected in the same manner.

There is evidence that transfecting cells with plasmids encoding MAL leads to an increase in MAL nuclear accumulation, because the overexpression of MAL relative to actin affects its regulation[71]. However, Scharenberg et al. transfected HEK293 cells with plasmids encoding MAL (thereby leading to MAL overexpression), serum starved these cells with serum-free DMEM for 20 hours, and consistently achieved low levels of MAL nuclear localisation[69]. So, whilst the overexpression of MAL caused by transfecting cells with the MAL reporter plasmid likely affects cell behaviour, serum starvation would still be expected to effectively reduce MAL nuclear localisation. All the HEK293T/17 cells used in the experiments described in this chapter were transfected with the same amounts of the same MAL reporter plasmid, and there were still significant differences between cells in the same condition.

HEK293T/17 cells are a subtype of HEK293T cells, which in turn are a subtype of HEK293 cells, selected for their ability to be efficiently transfected and produce protein and viral particles[72]. There are significant differences between different HEK293 subtypes, in terms of their genomic structure and transcriptome, especially in cytoskeletal genes[73]. I was unable to find any studies investigating MAL specifically in HEK293T/17 cells, so it could be that the changes in this HEK293 subtype have affected pathways which interfere with the normal regulation and subcellular localisation of MAL. It could also be that mutations arose during routine passaging of these cells in the lab, which affected MAL nuclear accumulation in subsequent experiments. Cells were kept between 10 and 20 passages and routinely thawed from frozen to reduce the risk of mutations arising, but whole genome sequencing would have been required to determine whether mutations had occurred. Another frequent issue in cell culture is mycoplasma infection, which can influence many aspects of cell behaviour, including signal transduction, gene expression, and cell morphology[74]. Disturbances in these cellular processes would likely affect MAL but, due to time and resource constraints, I was unable to test for mycoplasma infection.

Finally, since MAL is a key part of several different cell signalling pathways which can respond to a wide range of external stimuli, changes in different batches of media, serum, and

other reagents used to maintain, transfect, and infect cells could have contributed to the differences in MAL subcellular localisation.

In conclusion, infecting HEK293T/17 cells transfected with a MAL reporter plasmid with *B. quintana* seemed an efficient way to assess the effect of the bacteria on MAL's subcellular localisation but did not yield any reliable results. I was unable to achieve a consistent baseline for MAL nuclear localisation in serum-starved cells and could not identify the cause of the significant variation that occurred between experiments. HEK293T/17 cells are derived from kidney cells, which are not thought to be as relevant to *B. quintana* infection as other cell types such as immune and endothelial cells[73]. Therefore, this model was not used for any subsequent experiments. Instead, I developed a model using a human immune cell line, which better represent the types of cells *B. quintana* interacts with during its infection cycle.

Chapter 4 - Investigating the effects of *B. quintana* on MAL in THP-1 cells

4.1 Introduction

Bartonella have been shown to interact with host macrophages and modulate immune responses, cell migration, and proliferation[24,75,76]. Cell migration involves cytoskeletal changes regulated by the MAL/SRF pathway, and MAL has been shown to be important to the migration of several types of immune cells[33,61]. Additionally, in macrophages, MAL has been shown to be an important mediator of NF-κB-dependent proinflammatory responses[58,59,77,78]. Since there is evidence that *B. quintana* affects cell migration and immune responses in macrophages and MAL is part of signalling axes which contribute to the regulation of both these cellular processes, *B. quintana* could affect MAL in macrophages. To investigate this, THP-1 cells (a human monocytic cell line used as a model for human macrophages) were infected with GFP-*B. quintana* and stained with antibodies against MAL. Fluorescence microscopy was then used to measure differences in MAL's subcellular localisation, allowing the effect of *B. quintana* on MAL to be determined.

Detecting endogenous MAL using antibody staining has several advantages over using a MAL reporter plasmid. It removes the need for transfection, which leads to MAL overexpression and the introduction of double-stranded DNA into the cell, both of which can affect normal cell behaviour. A fluorescent strain of *B. quintana* was used, allowing the bacteria to be visualised using fluorescence microscopy and the interactions between *B. quintana* and host cells to be explored.

Previous experiments with THP-1 cells have shown that LPS activates MAL via TLR4 signalling, causing it to accumulate in the nucleus and interact with NF-κB to drive the expression of proinflammatory genes[58]. I was unable to find any previous studies describing the effects of serum, or other known activators of the MAL/SRF pathway, in THP-1 cells. Whilst LPS may not activate the MAL/SRF pathway in THP-1 cells, it is still expected to activate MAL and induce its nuclear accumulation. Therefore, I used LPS as a positive control for MAL nuclear accumulation in THP-1 cells. I couldn't find information on the effects of serum starvation on MAL in THP-1 cells in the literature, but since serum-free media does not contain any factor known to activate the MAL/SRF pathway or the LPS-TLR4-MAL-NF-κB signalling axis, serum starvation was used as a negative control for MAL

nuclear accumulation. By comparing the levels of MAL nuclear localisation in THP-1 cells infected with *B. quintana* to serum-starved cells and LPS-stimulated cells, the effect of *B. quintana* on MAL can be determined, even if the specific MAL pathway involved cannot be identified.

4.2 Results

4.2.1 Investigating the effects of LPS and *B. quintana* on MAL

To investigate the effects of *B. quintana* and LPS on MAL's subcellular localisation in THP-1 cells, THP-1 cells were seeded onto coverslips and differentiated into macrophage-like cells using PMA. After 24 hours of serum starvation in serum-free RPMI, cells were infected with GFP-*B. quintana* at MOI 100 for 90 minutes and then stimulated with 100 ng/mL of LPS for 0 – 3 hours. Uninfected cells were also stimulated with LPS. The results of three independent experiments are shown in Figure 4.1.

The data presented in Figure 4.1 showed that MAL nuclear accumulation was significantly affected by LPS stimulation ($p<0.0001$) and *B. quintana* infection ($p<0.0001$). In uninfected cells (MOI 0), 1, 2, and 3 hours of LPS treatment significantly increased the percent of cells with nuclear MAL compared to serum-starved unstimulated cells ($p<0.0001$ for all comparisons). There were no significant differences in MAL nuclear localisation between 1, 2, and 3 hours of LPS stimulation. In infected cells (MOI 100), 1 and 2 hours of LPS treatment significantly increased MAL nuclear accumulation compared to infected unstimulated cells ($p=0.0257$, and $p=0.0049$, respectively). However, 3 hours of LPS treatment did not significantly increase MAL nuclear accumulation. Comparing unstimulated uninfected cells to unstimulated infected cells (MOI 0 0 h LPS vs MOI 100 0 h LPS), showed that infected cells had significantly higher levels of nuclear MAL than uninfected cells ($p<0.0001$). The levels of nuclear MAL in infected and uninfected cells at 1, 2, and 3 hours of LPS stimulation were not significantly different.

Overall, Figure 4.1 shows that stimulating THP-1 cells with LPS for 1, 2, or 3 hours induces nuclear accumulation of MAL, as expected, and that *B. quintana* infection, prior to the addition of LPS, increases MAL nuclear accumulation at a MOI of 100.

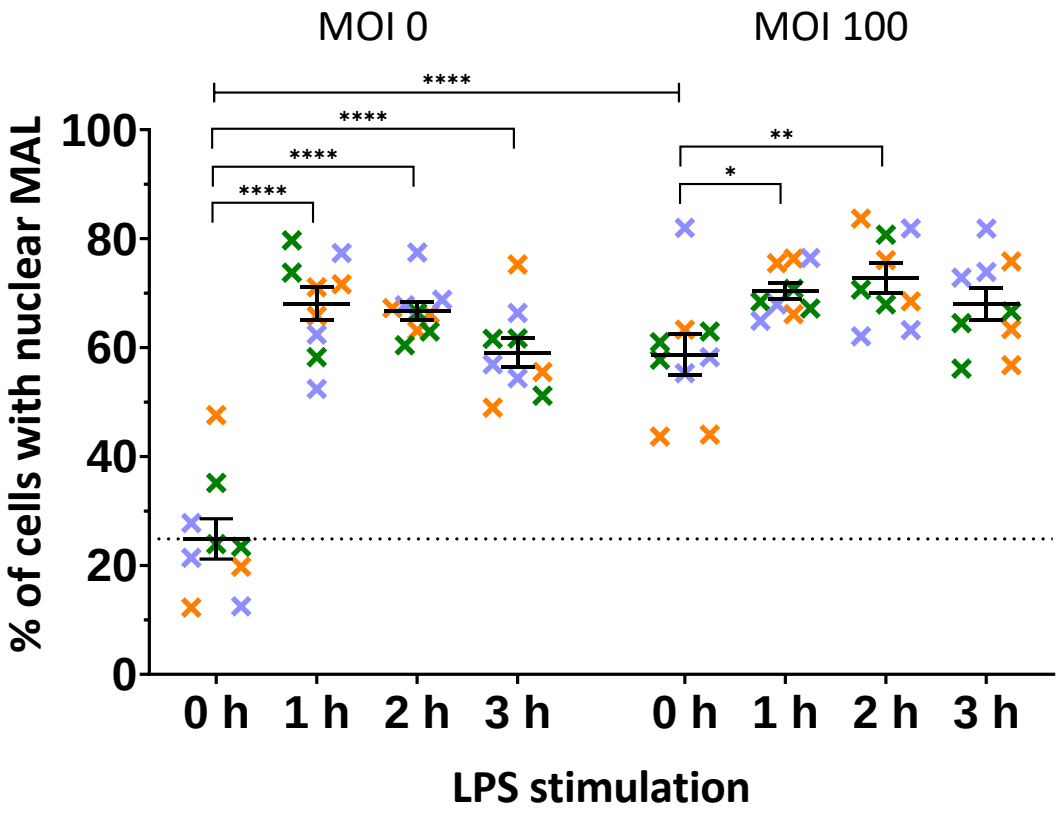

Figure 4.1: Effect of *B. quintana* and LPS on MAL nuclear localisation in THP-1 cells. Each data point corresponds to one biological replicate, with the three different colours representing three independent experiments. Error bars represent the mean and SEM. The dotted line represents the mean percent of cells with nuclear MAL in the negative control (MOI 0 0 h LPS). *p<0.05; **p<0.01; ***p<0.001; ****p<0.0001. Two-way ANOVA with Tukey's multiple comparisons tests (for comparing different timepoints with the same MOI) and Sidak's multiple comparisons tests (for comparing different MOIs with the same timepoint). Non-significant differences are not shown.

4.2.2 Investigating the dose-dependent effect of *B. quintana* on MAL

The results described in Figure 4.1 suggested that infection with *B. quintana* at a MOI of 100 is sufficient to induce MAL nuclear localisation in THP-1 cells, but not whether lower MOIs can also achieve comparable levels of MAL nuclear accumulation, or whether higher MOIs lead to greater levels of nuclear MAL. Therefore, the dose-dependent effect of *B. quintana* on MAL nuclear accumulation in THP-1 cells was investigated by infecting cells with eight different MOIs ranging from 0 to 1000. Cells were serum starved for 24 hours, infected with GFP-*B. quintana* for 90 minutes, then fixed, stained for DNA and actin, mounted onto slides, and imaged. The results of one experiment are shown in Figure 4.2.

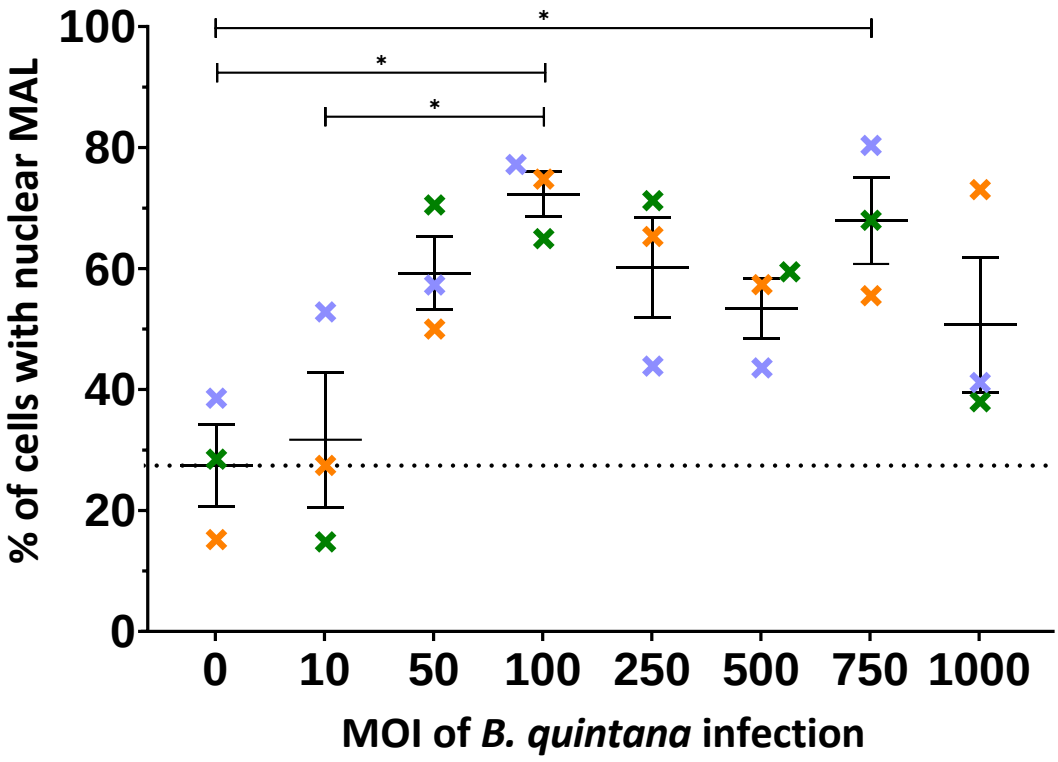

Figure 4.2: Dose-dependent effect of *B. quintana* on MAL nuclear localisation in THP-1 cells. Each data point corresponds to one biological replicate, with the three different colours representing different biological replicates. Error bars represent the mean and SEM. The dotted line represents the mean percent of cells with nuclear MAL in the negative control (MOI 0). *p<0.05. One-way ANOVA with Tukey's multiple comparisons tests. Non-significant differences are not shown.

Figure 4.2 shows that the MOI of *B. quintana* infection significantly affects MAL nuclear localisation (p=0.0084). Compared to uninfected cells, cells infected with *B. quintana* at MOIs of 100 and 750 had significantly greater levels of nuclear MAL (p=0.0162, and p=0.0347, respectively). Compared to cells infected with a MOI of 10, cells infected with a MOI of 100 had significantly increased MAL nuclear localisation (p=0.0342). There were no other significant differences in MAL nuclear accumulation between different MOIs. Whilst Figure 4.2 does not show that the percent of cells with nuclear MAL increases as the MOI increases, there are significant differences between uninfected cells and some of the MOIs tested, suggesting that *B. quintana* does affect MAL in THP-1 cells. Due to time constraints, and issues with *B. quintana* culture, this experiment could not be replicated.

4.2.3 Visualising the interactions between *B. quintana* and THP-1 cells

Several secreted *Bartonella* effectors, Beps, have been shown to cause actin rearrangements, such as membrane ruffle formation, so THP-1 cells were infected with GFP-*B. quintana* and stained for actin to visualise the interactions between *B. quintana* and the host cytoskeleton[30]. A representative image of a THP-1 cell infected with GFP-*B. quintana* is shown in Figure 4.3. Whilst GFP-*B. quintana* can be seen, the microscopy tools available were not able to detect specific interactions between host actin and GFP-*B. quintana*, or to differentiate between intracellular and extracellular bacteria.

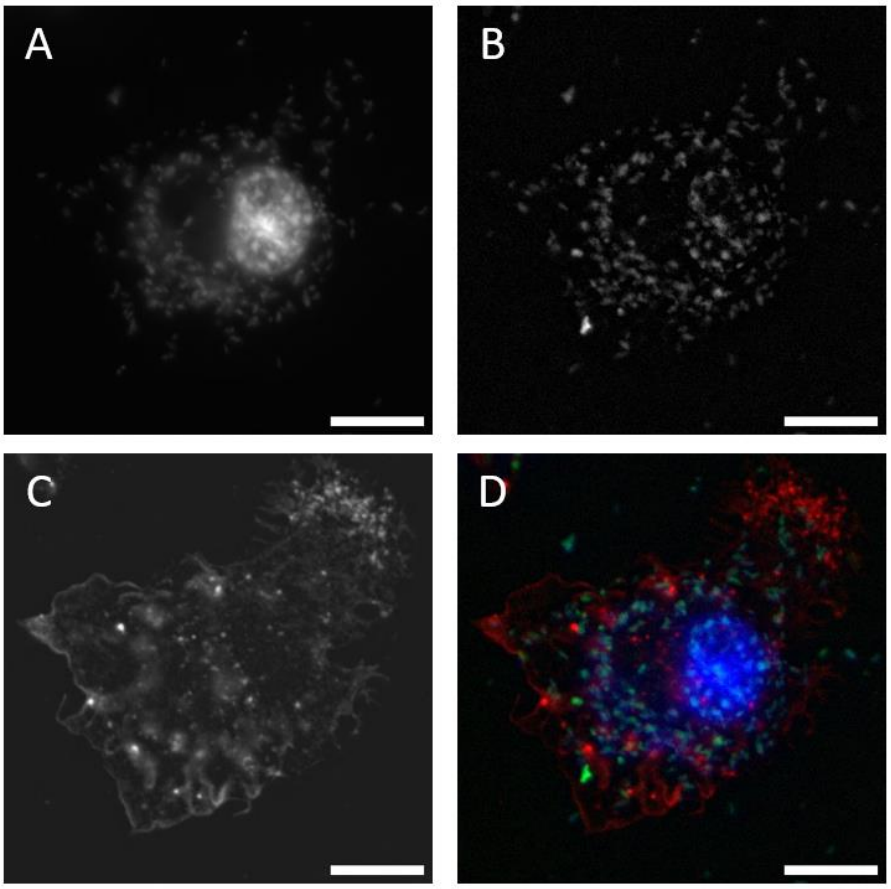

Figure 4.3: GFP-*B. quintana* infecting a THP-1 cell. Microscopy images showing a THP-1 cell infected with GFP-*B. quintana* at a MOI of 1000. Images were taken at 100× magnification and scale bars represent 10 µm. A: DNA stained with DAPI. B: GFP-*B. quintana*. C: F-actin stained with Alexa Fluor™ 647-phalloidin. D: composite image with actin in red, DNA in blue, and GFP-*B. quintana* in green. GFP-*B. quintana* can be seen as small rods in the DAPI and GFP channels.

4.3 Discussion

The aim of the experiments described in this chapter was to determine whether *B. quintana* affects MAL in THP-1 cells. This was investigated by differentiating THP-1 cells into macrophage-like cells, infecting them with GFP-*B. quintana*, and then staining cells with antibodies to detect MAL. By comparing the subcellular localisation of MAL in THP-1 cells in response to LPS stimulation (a known inducer of MAL nuclear localisation), serum

starvation (an established negative control for MAL nuclear localisation), and infection with *B. quintana*, we found that at a MOI of 100 *B. quintana* induces MAL nuclear localisation. Varying the MOI of *B. quintana* infection did not affect the level of MAL nuclear accumulation in a dose-dependent manner, but more experimental replicates would be needed to confirm this result.

LPS stimulation was used as a positive control since previous studies showed that it induced MAL nuclear accumulation in THP-1 cells[58]. However, LPS exerts its effects on cells via TLR4 signalling, and *B. quintana*'s LPS has been shown to be a potent TLR4 antagonist[79]. This suggests that the significant increases in MAL nuclear localisation observed in THP-1 cells infected with *B. quintana* are mediated by a host signalling pathway independent of TLR4.

Figure 4.1 shows that in infected cells, LPS stimulation is still correlated with increased MAL nuclear localisation. This could be because there is not enough *B. quintana* LPS present to completely block all TLR4 signalling, and thus *E. coli* LPS still induces MAL nuclear localisation in the presence of *B. quintana*. It could also be that the observed increases in nuclear MAL are not due to LPS stimulation, but due to longer incubation with *B. quintana*. During this experiment, cells were infected with *B. quintana* for 90 minutes, and then LPS media was added to the cells (without removing *B. quintana*-containing media) for an additional 1, 2, and 3 hours. It would be worthwhile to supplement these data with an additional experiment, infecting THP-1 cells with *B. quintana* at a MOI of 100 for 150 minutes, 210 minutes, and 270 minutes, and then comparing the levels of nuclear MAL at these timepoints to the levels of nuclear MAL in infected cells at 1 h, 2 h, and 3 h of LPS stimulation. If similar increases in MAL nuclear localisation are observed, then the effect shown in Figure 4.1 is likely due to *B. quintana*, and not LPS. However, if cells infected with *B. quintana* have less MAL nuclear accumulation than cells that have been infected and stimulated with LPS, then LPS signalling is likely still driving MAL's nuclear accumulation, indicating there is not enough *B. quintana* LPS present to completely block TLR4 signalling. Testing shorter and longer timepoints of *B. quintana* infection without LPS stimulation would also determine how quickly *B. quintana* causes MAL nuclear accumulation and how long this effect lasts.

LPS stimulation of macrophages leads to a NF-κB-dependent proinflammatory response, characterised by the release of cytokines such as IL-1 and IL-6[58,78]. In contrast, *B. quintana*

LPS does not induce IL-6 secretion in primary human macrophages, and instead prevents *E. coli* LPS from activating TLR4 and stimulating cytokine production[79]. ELISA assays could be used to measure the levels of proinflammatory cytokines (such as IL-1, TNF-α, and IL-6) and anti-inflammatory cytokines (such as IL-10) to determine if LPS and *B. quintana* drive different inflammatory responses in THP-1 cells.

Whilst the effect of *B. quintana* LPS on TLR4 signalling has been characterised, little is known about the interactions of *B. quintana* with other pattern recognition receptors (PRRs) such as TLR2. There is evidence that *Bartonella* can induce cell immune responses via TLR2, but the link between TLR2 and MAL is largely unknown[80,81]. To investigate this, THP-1 cells could be stimulated with known TLR2 agonists, such as Omp16 and Omp19 from *Brucella* species, to determine whether TLR2 signalling induces MAL nuclear localisation[81]. If this is found to be the case, TLR2 signalling in THP-1 cells could be inhibited (e.g., by mutating the genes coding for TLR2 or using antagonists to block the receptor) and these cells could be infected with *B. quintana*. The effects of *B. quintana* on MAL nuclear localisation in THP-1 cells with normal and impaired TLR2 signalling could then be compared. Since multiple cell surface receptors and signalling cascades can activate MAL to direct both pro- and anti-inflammatory responses, it would be valuable to identify the type of inflammatory response that occurs in THP-1 cells in response to *B. quintana*, and the receptors that are activated during this process[82].

The nuclear accumulation of MAL is a useful proxy for MAL activation, but studies have shown that MAL can accumulate in the nucleus without affecting gene expression[39,51]. This is due to post-translational modifications of MAL, as well as its interactions with nuclear actin and other nuclear proteins, which influence MAL's ability to bind DNA[39,40,42]. As a transcription cofactor, MAL regulates gene expression by binding transcription factors, such as SRF and NF-κB, and enhancing their ability to bind the promoters of target genes[31,77]. It would therefore be worthwhile to confirm *B. quintana* not only leads to increased nuclear accumulation of MAL, but also increases its binding to transcription factors. This could be explored using co-immunoprecipitation assays. Antibodies against SRF and NF-κB could be used to isolate these proteins from infected and uninfected cells, and the amount of MAL bound to the two transcription factors could be quantified using Western blots. Not only would this confirm activation of MAL, it would also determine whether *B. quintana* modulates MAL to drive SRF or NF-κB activation.

Once the specific cell signalling pathway activated by MAL in response to *B. quintana* has been identified, luciferase assays could be used to examine how *B. quintana* affects signalling downstream of MAL. THP-1 cells could be transfected with NF-κB or SRF luciferase reporter constructs, and luciferase activity in response to *B. quintana* could be measured. This would confirm that the increase in MAL nuclear localisation caused by *B. quintana* correlates with changes in SRF or NF-κB signalling.

There is evidence that *Bartonella* disturb host cell actin structures, so I aimed to visualise the interactions between GFP-*B. quintana* and the host cell cytoskeleton using fluorescence microscopy. Images such as the one shown in Figure 4.3 suggest that *B. quintana* are interacting with THP-1 cells, however live cell microscopy might be better suited to investigate these interactions. Cells could be stained with a live-cell tracking stain for actin, infected with GFP-*B. quintana,* and visualised at different timepoints during infection. If structures such as membrane ruffles or phagosomes are observed in response to *B. quintana,* then the molecular mechanisms involved would need to be characterised with further experiments.

Overall, the results presented in this chapter suggest that *B. quintana* activates MAL in THP-1 cells, but further research is needed to confirm that the increased levels of nuclear MAL result in increased MAL activity, determine whether SRF or NF-κB is involved, and to identify the functional consequences of *B. quintana*-dependent MAL activation.

Chapter 5 - Discussion

5.1 Research motivation

Mammalian cell signalling is complex, with many pathways interacting to fine-tune a diverse range of cellular processes. *B. quintana* is a pathogen highly adapted to the human host, which subverts host signalling pathways in order to disseminate throughout the body, avoid immune responses, and establish a long-term infection[24]. The specific molecular mechanisms by which *B. quintana* modulates host cell behaviour are largely unknown. Many studies of *Bartonella* pathogenesis focus on species such as *B. henselae* and *B. tribocorum*, which do not infect humans as a reservoir host[24]. However, it has become clear that even though *Bartonella* species share similar infection strategies and conserved Bep sequences, Bep-host cell interactions depend on both the *Bartonella* species and the host species[29,30]. Therefore, to fully understand how *B. quintana* establishes an infection in a human host, studies investigating the interactions between *B. quintana* and human cells are essential.

This research project aimed to determine whether *B. quintana* activates the transcriptional cofactor MAL in human cells. MAL is a key regulator of the SRF and NF-κB pathways, which affect cell cytoskeletal regulation and immune responses, respectively. Since there is evidence that *B. quintana* modulates these cellular processes and *B. quintana* Beps have been shown to target known activators of MAL, we hypothesized that *B. quintana* would influence MAL.

To investigate the effect of *B. quintana* on MAL, I developed tissue culture models that enabled the subcellular localisation of MAL, which is correlated to MAL's activity, to be visualised using fluorescence microscopy. By comparing the percent of cells with nuclear MAL in infected and uninfected host cells, I was able to assess the effect of *B. quintana* on MAL.

5.2 Key findings

The first model I developed involved transfecting HEK293T/17 cells with a MAL reporter plasmid and comparing the nuclear localisation of MAL-mCherry in infected and uninfected cells. This method seemed a promising way to rapidly perform high-throughput experiments testing a range of infection conditions. However, I was unable to generate a consistent baseline for MAL-mCherry nuclear localisation in transfected HEK293T/17 cells. Therefore,

from the experiments carried out using this model, I was unable to determine whether *B. quintana* affected MAL.

I developed a second model using THP-1 cells and antibody staining to visualise MAL's subcellular localisation. Using serum starvation and LPS stimulation as negative and positive controls for MAL nuclear accumulation, I observed expected low and high levels of nuclear MAL, respectively. I then infected THP-1 cells with *B. quintana* and found that infection with *B. quintana* increases MAL's nuclear localisation at certain MOIs. This suggests that *B. quintana* affects MAL in human macrophages, potentially to modulate MAL/SRF signalling or MAL/NF-κB signalling.

5.3 Future directions

Whilst these results are promising, more work is required to identify the signalling axis by which *B. quintana* induces MAL nuclear accumulation, the cellular processes affected by this pathway, and how this contributes to *B. quintana*'s infection strategy.

5.3.1 Identifying the *B. quintana* factors that affect MAL

B. quintana could affect MAL in several different ways. *B. quintana* factors, such as outer membrane proteins, could activate host cell pattern recognition receptors, triggering an immune response that activates MAL. Alternatively, *B. quintana* could inject effector proteins into host cells that actively target components of signalling pathways involved in the regulation of MAL.

Many *Bartonella*-mediated modulations of cell signalling are thought to be driven by Beps, which are translocated into host cells via the VirB/VirD4 T4SS[2]. For instance, *B. quintana* BepC activates F-actin stress fibre formation in host cells and BepE can induce membrane ruffle and filopodia formation[29,30]. To determine whether the effect of *B. quintana* on MAL nuclear localisation is regulated by Beps, cells could be infected with *B. quintana* lacking a functional VirB/VirD4 T4SS. This can be achieved by knocking out genes that code for essential components of the VirB/VirD4 T4SS, such as the VirB4 subunit, from *B. quintana*[24]. THP-1 cells could be infected with this mutant strain, using the same experimental design described in Chapter 4, to determine if the lack of a functional VirB/VirD4 T4SS affects *B. quintana*'s ability to induce MAL nuclear localisation. If this is the case, the specific Bep involved could be identified by cloning different *B. quintana* Bep genes into mammalian expression plasmids, transfecting THP-1 cells with these plasmids and identifying any

resulting effects on the nuclear localisation of MAL. This would uncover which *B. quintana* Bep, or Beps, drives MAL nuclear accumulation in THP-1 cells.

B. quintana's effect on MAL could also be mediated by factors other than Beps. For example, *Bartonella* angiogenic factor A (BafA) secreted by *B. henselae* and *B. quintana* has been shown to interact with host cell surface receptors, thereby activating downstream signalling pathways that drive cell proliferation and the expression of angiogenesis-related genes[83]. To determine whether *B. quintana* affects the nuclear accumulation of MAL via a secreted factor, THP-1 cells could be treated with *B. quintana* using indirect co-culture so that secreted bacterial proteins, but not bacterial cells, can interact with the host cells. This technique has been previously used to determine whether the effect of *B. henselae* on HUVECs required the bacteria to contact the host cells[83]. If indirect culture with *B. quintana* leads to increased MAL nuclear localisation in THP-1 cells, then this effect is likely mediated by a secreted factor, such as BafA.

There is evidence that *B. quintana* variable outer membrane proteins (Vomps) can stimulate host cells to secrete VEGF, so Vomps could be mediating the effect of *B. quintana* on MAL[84]. The JK-31 *B. quintana* strain used in this project expresses VompA, B, and C, however the *B. quintana* strain 2-D70 does not express any of these proteins[84]. If the effect of *B. quintana* on MAL is Vomp-dependent, no increase in nuclear MAL would be observed in THP-1 cells infected with a *B. quintana* strain such as 2-D70.

5.3.2 Identifying the link between *B. quintana* and MAL signalling

It remains to show which cell signalling components upstream of MAL are affected by *B. quintana*. There is evidence that *B. quintana* targets the host RhoA/ROCK pathway, which is known to regulate MAL[23,29]. Pre-treating cells with Rho/ROCK pathway inhibitors (such as Y27632, which specifically inhibits ROCK1 and ROCK2) prior to infection would determine whether *B. quintana* induces MAL nuclear localisation via Rho signalling or not[85].

Many different proteins can act on actin and RhoA to influence MAL. If the effect of *B. quintana* on MAL nuclear localisation was found to be Rho-dependent, the specific components required could be identified.

A study of EPEC found that actin-binding Rho-activating protein (ABRA) was essential for the nuclear accumulation of MAL in response to bacterial infection[64]. ABRA, also called striated muscle activator of Rho signalling (STARS), is expressed in cardiac and skeletal

muscle and has been shown to activate the MAL/SRF pathway in an actin-dependent manner[64,86,87]. Previous work in the lab suggests that Myozap could be targeted by *B. quintana* BepA1[70]. Myozap is a recently identified intercalated disc protein which can activate the SRF pathway via RhoA[88–90]. Whilst ABRA and Myozap are involved in activation of MAL signalling and are potentially targeted by bacterial factors, there is no evidence of either protein being expressed in immune cells. It would be worthwhile to confirm the lack or presence of ABRA and Myozap in THP-1 cells, by using Western blots to examine protein expression and RT-PCR experiments to determine if the THP-1 transcriptome contains transcripts coding for these two proteins. If ABRA and Myozap are indeed not expressed in THP-1 cells, then the effect of *B. quintana* on MAL must be occurring via other pathways.

If the *B. quintana* factor that affects MAL in THP-1 cells is identified, this bacterial factor could be used as the bait protein in a yeast two-hybrid assay against a library of host cell proteins, to identify potential binding partners.

Once the potential target of *B. quintana* is identified, it will remain to show how *B. quintana* affects this target. Many Beps contain filamentation induced by cAMP (FIC) domains, which AMPylate target proteins such as small GTPases to subvert host cell signalling[7,26]. Beps can also contain pY motifs (tyrosine residues that can be phosphorylated) which are recognised and phosphorylated by host cell kinases, thus allowing Beps to interact with host cell proteins that contain SH2 domains[7]. Proteins with SH2 domains are often involved in signalling cascades[91]. Some *B. henselae* Beps have been shown to be phosphorylated at tyrosine residues by host kinases and interact with SH2-containing proteins that can activate pathways involved in actin, inflammation, and cell proliferation[91]. Other post-translational modifications, such as acetylation and SUMOylation, can affect the function of host cell signalling proteins[55,92]. In order to explore the effects of *B. quintana* on cell signalling upstream of MAL, putative target proteins could be purified from infected and uninfected cells, or cells infected with wildtype and mutant *B. quintana*, and mass spectrometry could be used to identify any post-translational modifications resulting from *B. quintana* infection. Mass spectrometry could also be used to determine whether Beps recovered from infected host cells have been phosphorylated by host cell kinases. Once potential sites of post-translational modification have been identified, their functional role in *B. quintana*'s effect on host cell signalling would need to be confirmed, by mutating target residues and determining whether this influences *B. quintana*'s effect on MAL.

5.3.3 Investigating the effects of *B. quintana* on THP-1 cell migration

Several bacterial effectors, including Beps, can affect the actin cytoskeleton by activating Rho signalling to drive stress fibre formation[29,62]. The formation of stress fibres can be regulated by MAL/SRF signalling, and leads to changes in cell adhesion, structure, and migration[45]. So, *B. quintana*-mediated activation of MAL could induce changes in cell migration, potentially allowing the bacteria to use infected macrophages to disseminate within the host to the bloodstream. *B. quintana* has been shown to stimulate HUVEC migration through a porous membrane[93]. The effects of *B. quintana* on THP-1 migration could be investigated using transwell assays. This could involve comparing the ability of *B. quintana*-infected and uninfected THP-1 cells to migrate through porous membranes in response to VEGF, which has been shown to stimulate THP-1 migration in transwell assays[94]. If infected THP-1 cells had increased migration compared to uninfected cells in conditions without VEGF (i.e., in the absence of a factor driving migration) then this would suggest that *B. quintana* drives migration in THP-1 cells. MAL could then be silenced in THP-1 cells using siRNA and the experiment repeated, to determine whether *B. quintana*'s effect on THP-1 migration is MAL-dependent. Transmission electron microscopy (TEM) could be used to confirm the presence of intracellular *B. quintana* in migrating THP-1 cells.

5.3.4 Investigating the effect of *B. quintana* on MAL in different cell types

Both *B. quintana* and MAL have different effects on cell signalling in different cell types. Whilst we showed that *B. quintana* induced MAL nuclear accumulation in THP-1 cells, it would be worthwhile to replicate these experiments using different cell types. There is evidence that *Bartonella* invade dendritic cells (DCs) and affect their migration in order to disseminate through the dermis[23,24]. *Bartonella* can modulate endothelial cell responses to stimulate proliferation and angiogenesis, and previous studies have shown that Beps can induce actin rearrangements, NF-κB activation, and inhibit apoptosis in endothelial cells[2,76]. Since cell proliferation and angiogenesis can be regulated by the MAL/SRF pathway, and MAL can also regulate NF-κB signalling in different cell types, the effects of *B. quintana* on these cellular processes in endothelial cells potentially involve changes in MAL's subcellular localisation and activity[58,95]. It would be interesting to compare the effect of *B. quintana* on MAL nuclear localisation in DCs and endothelial cells to the effect observed in THP-1 cells.

5.3.5 Exploring the effects of *B. quintana* on epigenetic modifications

Research in a range of fields, including cancer, cardiac disease, inflammation, and immunity, indicates that MAL is an important epigenetic regulator in many cell types[77,92,96,97]. Many of MAL's epigenetic effects involve the complex of proteins associated with Set1 (COMPASS)[98]. COMPASS catalyses histone H3K4 methylation, which is associated with active chromatin and increased gene expression[99]. In THP-1 cells, MAL's recruitment of members of the COMPASS complex to the promoters of NF-κB target genes and the resulting epigenetic modifications are essential to NF-κB-dependent inflammation in response to LPS and TNF-α[58,59,78]. In HUVECs, increased expression of VE-cadherin in response to VEGF involves interactions between the histone acetyltransferase (HAT) p300 and MAL at the SRF-binding site in the VE-cadherin promoter[100]. By mediating interactions between SRF and HATs at the CCN1 promoter (a proangiogenic gene), MAL drives the expression of CCN1 and thus contributes to angiogenesis[51,92]. In macrophages, MAL regulates epigenetic modifications at the iNOS promoter which allow NF-κB to bind and induce iNOS expression[101]. oxLDL-driven expression of ICAM-1 in endothelial cells involves epigenetic modifications regulated by MAL and interactions between SRF, MAL, and NF-κB at the ICAM-1 promoter[102]. In hepatic stellate cells, MAL can recruit COMPASS proteins to the promoters of profibrogenic genes and contribute to liver fibrosis[103].

There is evidence that *Bartonella* species induce NF-κB-dependent inflammatory responses, iNOS and ICAM-1 expression, angiogenesis, and affect host liver cells[9,53,76,104,105]. Since MAL can affect these cellular pathways by regulating epigenetic modifications, and this project suggests that *B. quintana* infection influences MAL, *B. quintana* could modulate host epigenetic modifications via MAL. This could be investigated by using ChIP-qPCR experiments to quantify differences in the binding of key epigenetic enzymes (e.g. members of the COMPASS complex) to the promoters of MAL/SRF and MAL/NF-κB target genes in response to *B. quintana* infection. This could potentially uncover a novel mechanism by which *B. quintana* modulates host cell gene expression and contribute to our understanding of epigenetic regulation in mammalian cells.

Many of MAL's epigenetic effects are associated with diseases such as fibrosis, cancer, and cardiovascular disease[96,102,103,106,107]. If *B. quintana*'s effect on MAL is found to involve epigenetic changes and the specific effector proteins involved are identified, then these effectors could be used to develop treatments for diseases that result from excessive MAL

signalling. Similarly, epigenetic drugs could be used to counter any adverse epigenetic modifications that result from *B. quintana* infection. Epigenetic therapies are still developing, but offer a promising way to treat disease since they can be used to induce specific and reversible changes in gene expression[108].

5.4 Concluding remarks

In conclusion, the work presented in this thesis suggests that *B. quintana* affects the host transcriptional cofactor MAL. The molecular mechanisms by which *B. quintana* interacts MAL and the functional consequences of this interaction remain to be uncovered. Future research into these areas could lead to the development of novel treatments of *B. quintana* infection and expand our understanding of cell biology.

Bibliography

1. Parte, A. C., Carbasse, J. S., Meier-Kolthoff, J. P., Reimer, L. C. & Göker, M. List of Prokaryotic names with Standing in Nomenclature (LPSN) moves to the DSMZ. *Int. J. Syst. Evol. Microbiol.* **70**, 5607–5612 (2020).

2. Dehio, C. Infection-associated type IV secretion systems of *Bartonella* and their diverse roles in host cell interaction. *Cell. Microbiol.* **10**, 1591–1598 (2008).

3. McKee, C. D., Bai, Y., Webb, C. T. & Kosoy, M. Y. Bats are key hosts in the radiation of mammal-associated *Bartonella* bacteria. *Infect. Genet. Evol.* **89**, 104719 (2021).

4. Bisch, G. *et al.* Genome Evolution of Bartonellaceae Symbionts of Ants at the Opposite Ends of the Trophic Scale. *Genome Biol. Evol.* **10**, 1687–1704 (2018).

5. Breitschwerdt, E. B. Bartonellosis: one health perspectives for an emerging infectious disease. *ILAR J.* **55**, 46–58 (2014).

6. Segers, F. H., Kešnerová, L., Kosoy, M. & Engel, P. Genomic changes associated with the evolutionary transition of an insect gut symbiont into a blood-borne pathogen. *ISME J.* **11**, 1232–1244 (2017).

7. Wagner, A. & Dehio, C. Role of distinct type-IV-secretion systems and secreted effector sets in host adaptation by pathogenic *Bartonella* species. *Cell. Microbiol.* **21**, (2019).

8. Hang, J. *et al.* Complete Genome Sequence of *Bartonella ancashensis* Strain 20.00, Isolated from the Blood of a Patient with Verruga Peruana. *Genome Announc.* **3**, (2015).

9. Minnick, M. F. & Anderson, B. E. Chapter 105 - *Bartonella*. in *Molecular Medical Microbiology (Second Edition)* (eds. Tang, Y.-W., Sussman, M., Liu, D., Poxton, I. & Schwartzman, J.) 1911–1939 (Academic Press, Boston, 2015). doi:10.1016/B978-0-12-397169-2.00105-0.

10. Harms, A. & Dehio, C. Intruders below the Radar: Molecular Pathogenesis of *Bartonella* spp. *Clin. Microbiol. Rev.* **25**, 42–78 (2012).

11. Ogrzewalska, M., Rozental, T., Favacho, A. R. M. & Monteiro de Mello Mares-Guia, M. A. Rickettsial Infections, Bartonella Infections, and Coxiellosis. in *Arthropod Borne Diseases* (ed. Marcondes, C. B.) 171–191 (Springer International Publishing, Cham, 2017). doi:10.1007/978-3-319-13884-8_12.

12. LeBoit, P. E. *et al.* Bacillary angiomatosis. The histopathology and differential diagnosis of a pseudoneoplastic infection in patients with human immunodeficiency virus disease. *Am. J. Surg. Pathol.* **13**, 909–920 (1989).

13. Cockerell, C. J. & LeBoit, P. E. Bacillary angiomatosis: A newly characterized, pseudoneoplastic, infectious, cutaneous vascular disorder. *J. Am. Acad. Dermatol.* **22**, 501–512 (1990).

14. Maurin, M. & Raoult, D. *Bartonella* (*Rochalimaea*) *quintana* infections. *Clin. Microbiol. Rev.* **9**, 273–292 (1996).

15. Kostrzewski, J. The epidemiology of trench fever. *Bull. Int. Acad. Pol. Sci. Lett. Cl. Med.* **7**, 233–263 (1949).

16. Foucault, C., Brouqui, P. & Raoult, D. *Bartonella quintana* Characteristics and Clinical Management. *Emerg. Infect. Dis. J.* **12**, 217–223 (2006).

17. Drancourt, M., Tran-Hung, L., Courtin, J., Lumley, H. de & Raoult, D. *Bartonella quintana* in a 4000-Year-Old Human Tooth. *J. Infect. Dis.* **191**, 607–611 (2005).

18. Mai, B.-H.-A. *et al.* Five millennia of *Bartonella quintana* bacteraemia. *PLOS ONE* **15**, (2020).

19. Barbieri, R. *et al.* A 2,000–year-old specimen with intraerythrocytic *Bartonella quintana*. *Sci. Rep.* **10**, (2020).

20. Deng, Y.-P. *et al.* Emerging bacterial infectious diseases/pathogens vectored by human lice. *Travel Med. Infect. Dis.* **55**, 102630 (2023).

21. Dehio, C. & Tsolis, R. M. Type IV Effector Secretion and Subversion of Host Functions by *Bartonella* and *Brucella* Species. in *Type IV Secretion in Gram-Negative and Gram-Positive Bacteria* (eds. Backert, S. & Grohmann, E.) vol. 413 269–295 (Springer, Cham, 2017).

22. Hong, J. *et al.* Lymphatic Circulation Disseminates *Bartonella* Infection Into Bloodstream. *J. Infect. Dis.* **215**, 303–311 (2017).

23. Okujava, R. *et al.* A Translocated Effector Required for *Bartonella* Dissemination from Derma to Blood Safeguards Migratory Host Cells from Damage by Co-translocated Effectors. *PLOS Pathog.* **10**, (2014).

24. Fromm, K. & Dehio, C. The Impact of *Bartonella* VirB/VirD4 Type IV Secretion System Effectors on Eukaryotic Host Cells. *Front. Microbiol.* **12**, (2021).

25. Schröder, G. & Dehio, C. Virulence-associated type IV secretion systems of *Bartonella*. *Trends Microbiol.* **13**, 336–342 (2005).

26. Harms, A. *et al.* Evolutionary Dynamics of Pathoadaptation Revealed by Three Independent Acquisitions of the VirB/D4 Type IV Secretion System in *Bartonella*. *Genome Biol. Evol.* **9**, 761–776 (2017).

27. Schmid, M. C. *et al.* A Translocated Bacterial Protein Protects Vascular Endothelial Cells from Apoptosis. *PLOS Pathog.* **2**, (2006).

28. Engel, P. *et al.* Parallel Evolution of a Type IV Secretion System in Radiating Lineages of the Host-Restricted Bacterial Pathogen *Bartonella*. *PLOS Genet.* **7**, e1001296 (2011).

29. Marlaire, S. & Dehio, C. *Bartonella* effector protein C mediates actin stress fiber formation via recruitment of GEF-H1 to the plasma membrane. *PLOS Pathog.* **17**, (2021).

30. Wang, C. *et al. Bartonella quintana* type IV secretion effector BepE-induced selective autophagy by conjugation with K63 polyubiquitin chain. *Cell. Microbiol.* **21**, (2019).

31. Cen, B., Selvaraj, A. & Prywes, R. Myocardin/MKL family of SRF coactivators: Key regulators of immediate early and muscle specific gene expression. *J. Cell. Biochem.* **93**, 74–82 (2004).

32. Miranda, M. Z., Lichner, Z., Szászi, K. & Kapus, A. MRTF: Basic Biology and Role in Kidney Disease. *Int. J. Mol. Sci.* **22**, 6040 (2021).

33. Sprenkeler, E. G. G., Guenther, C., Faisal, I., Kuijpers, T. W. & Fagerholm, S. C. Molecular Mechanisms of Leukocyte Migration and Its Potential Targeting—Lessons Learned From MKL1/SRF-Related Primary Immunodeficiency Diseases. *Front. Immunol.* **12**, 615477 (2021).

34. Du, H. *et al.* Tuning immunity through tissue mechanotransduction. *Nat. Rev. Immunol.* **23**, 174–188 (2023).

35. Wagner, A., Tittes, C. & Dehio, C. Versatility of the BID Domain: Conserved Function as Type-IV-Secretion-Signal and Secondarily Evolved Effector Functions Within *Bartonella*-Infected Host Cells. *Front. Microbiol.* **10**, (2019).

36. Wang, D.-Z. *et al.* Potentiation of serum response factor activity by a family of myocardin-related transcription factors. *Proc. Natl. Acad. Sci. U. S. A.* **99**, 14855 (2002).

37. Reed, F., Larsuel, S. T., Mayday, M. Y., Scanlon, V. & Krause, D. S. MRTFA: A critical protein in normal and malignant hematopoiesis and beyond. *J. Biol. Chem.* **296**, 100543 (2021).

38. Wang, D.-Z. *et al.* Activation of Cardiac Gene Expression by Myocardin, a Transcriptional Cofactor for Serum Response Factor. *Cell* **105**, 851–862 (2001).

39. Sidorenko, E. & Vartiainen, M. K. Nucleoskeletal regulation of transcription: Actin on MRTF. *Exp. Biol. Med. Maywood NJ* **244**, 1372–1381 (2019).

40. Vartiainen, M. K., Guettler, S., Banafshe, L. & Richard, T. Nuclear Actin Regulates Dynamic Subcellular Localization and Activity of the SRF Cofactor MAL. *Science* **316**, 1749–1752 (2007).

41. Miralles, F., Posern, G., Zaromytidou, A.-I. & Treisman, R. Actin Dynamics Control SRF Activity by Regulation of Its Coactivator MAL. *Cell* **113**, 329–342 (2003).

42. Panayiotou, R. *et al.* Phosphorylation acts positively and negatively to regulate MRTF-A subcellular localisation and activity. *eLife* **5**, 15460 (2016).

43. Burridge, K., Monaghan-Benson, E. & Graham, D. M. Mechanotransduction: from the cell surface to the nucleus via RhoA. *Philos. Trans. R. Soc. B Biol. Sci.* **374**, 20180229 (2019).

44. Settleman, J. A Nuclear MAL-Function Links Rho to SRF. *Mol. Cell* **11**, 1121–1123 (2003).

45. Tojkander, S., Gateva, G. & Lappalainen, P. Actin stress fibers – assembly, dynamics and biological roles. *J. Cell Sci.* **125**, 1855–1864 (2012).

46. Olson, E. N. & Nordheim, A. Linking actin dynamics and gene transcription to drive cellular motile functions. *Nat. Rev. Mol. Cell Biol.* **11**, 353–365 (2010).

47. Posern, G. & Treisman, R. Actin' together: Serum response factor, its cofactors and the link to signal transduction. *Trends Cell Biol.* **16**, 588–96 (2006).

48. Deshpande, A., Shetty, P. M. V., Frey, N. & Rangrez, A. Y. SRF: a seriously responsible factor in cardiac development and disease. *J. Biomed. Sci.* **29**, 38 (2022).

49. Yamamura, Y. *et al.* Myocardin-related transcription factor contributes to renal fibrosis through the regulation of extracellular microenvironment surrounding fibroblasts. *FASEB J.* **37**, e23005 (2023).

50. Liu, Z., Sun, J., Li, C., Xu, L. & Liu, J. MKL1 regulates hepatocellular carcinoma cell proliferation, migration and apoptosis via the COMPASS complex and NF-κB signaling. *BMC Cancer* **21**, 1184 (2021).

51. Hanna, M. *et al.* Mechanical Regulation of the Proangiogenic Factor CCN1/CYR61 Gene Requires the Combined Activities of MRTF-A and CREB-binding Protein Histone Acetyltransferase. *J. Biol. Chem.* **284**, 23125–23136 (2009).

52. Wang, N. *et al.* Vascular endothelial growth factor stimulates endothelial differentiation from mesenchymal stem cells via Rho/myocardin-related transcription factor-A signaling pathway. *Int. J. Biochem. Cell Biol.* **45**, 1447–1456 (2013).

53. Dehio, C. *Bartonella* interactions with endothelial cells and erythrocytes. *Trends Microbiol.* **9**, 279–285 (2001).

54. Oeckinghaus, A. & Ghosh, S. The NF-κB Family of Transcription Factors and Its Regulation. *Cold Spring Harb. Perspect. Biol.* **1**, a000034 (2009).

55. Kim, J.-G. *et al.* Regulation of RhoA GTPase and various transcription factors in the RhoA pathway. *J. Cell. Physiol.* **233**, 6381–6392 (2018).

56. Kustermans, G., Jamel, Piette, J. & Legrand-Poels, S. Perturbation of actin dynamics induces NF-κB activation in myelomonocytic cells through an NADPH oxidase-dependent pathway. *Biochem. J.* **387**, 531–540 (2005).

57. Pahl, H. L. Activators and target genes of Rel/NF-κB transcription factors. *Oncogene* **18**, 6853–6866 (1999).

58. Yu, L. *et al.* MKL1 defines the H3K4Me3 landscape for NF-κB dependent inflammatory response. *Sci. Rep.* **7**, 191 (2017).

59. Wenping, X., Quanyi, Z., Min, W., Mingming, F. & Yong, X. MKL1 mediates TNF-α induced pro-inflammatory transcription by bridging the crosstalk between BRG1 and WDR5. *J. Biomed. Res.* **33**, 164–172 (2019).

60. Sprenkeler, E. G. G. *et al.* MKL1 deficiency results in a severe neutrophil motility defect due to impaired actin polymerization. *Blood* **135**, 2171–2181 (2020).

61. Record, J. *et al.* Immunodeficiency and severe susceptibility to bacterial infection associated with a loss-of-function homozygous mutation of MKL1. *Blood* **126**, 1527–1535 (2015).

62. Popoff, M. R. Bacterial factors exploit eukaryotic Rho GTPase signaling cascades to promote invasion and proliferation within their host. *Small GTPases* **5**, (2014).

63. Kumar, A. *et al.* Essential role of Rnd1 in innate immunity during viral and bacterial infections. *Cell Death Dis.* **13**, 1–12 (2022).

64. Heath, R. J. W., Leong, J. M., Visegrády, B., Machesky, L. M. & Xavier, R. J. Bacterial and Host Determinants of MAL Activation upon EPEC Infection: The Roles of Tir, ABRA, and FLRT3. *PLOS Pathog.* **7**, (2011).

65. Schindelin, J. *et al.* Fiji: an open-source platform for biological-image analysis. *Nat. Methods* **9**, 676–682 (2012).

66. Gibson, D. G. *et al.* Enzymatic assembly of DNA molecules up to several hundred kilobases. *Nat. Methods* **6**, 343–345 (2009).

67. Benchling [Biology Software]. *Benchling* https://benchling.com (2023).

68. Addgene. Addgene: pcDNA3 mCherry LIC cloning vector (6B). https://www.addgene.org/30125/.

69. Scharenberg, M. A. *et al.* TGF-β-induced differentiation into myofibroblasts involves specific regulation of two MKL1 isoforms. *J. Cell Sci.* **127**, 1079–1091 (2014).

70. Lambert, C. Investigation of *Bartonella quintana* Host Immune Evasion. (Te Herenga Waka - Victoria University of Wellington, 2018).

71. Montel, L., Sotiropoulos, A. & Hénon, S. The nature and intensity of mechanical stimulation drive different dynamics of MRTF-A nuclear redistribution after actin remodeling in myoblasts. *PLOS ONE* **14**, e0214385 (2019).

72. Pear, W. S., Nolan, G. P., Scott, M. L. & Baltimore, D. Production of high-titer helper-free retroviruses by transient transfection. *Proc. Natl. Acad. Sci. U. S. A.* **90**, 8392–8396 (1993).

73. Malm, M. *et al.* Evolution from adherent to suspension: systems biology of HEK293 cell line development. *Sci. Rep.* **10**, 18996 (2020).

74. Drexler, H. G. & Uphoff, C. C. Mycoplasma contamination of cell cultures: Incidence, sources, effects, detection, elimination, prevention. *Cytotechnology* **39**, 75–90 (2002).

75. Kyme, P. A. *et al.* Unusual trafficking pattern of *Bartonella henselae*-containing vacuoles in macrophages and endothelial cells. *Cell. Microbiol.* **7**, 1019–1034 (2005).

76. Dehio, C. Recent progress in understanding *Bartonella*-induced vascular proliferation. *Curr. Opin. Microbiol.* **6**, 61–65 (2003).

77. Yu, L. *et al.* MRTF-A mediates LPS-induced pro-inflammatory transcription by interacting with the COMPASS complex. *J. Cell Sci.* **127**, 4645–4657 (2014).

78. Song, M. *et al.* MKL1 is an epigenetic mediator of TNF-α-induced proinflammatory transcription in macrophages by interacting with ASH2. *FEBS Lett.* **591**, 934–945 (2017).

79. Malgorzata-Miller, G. *et al. Bartonella quintana* lipopolysaccharide (LPS): structure and characteristics of a potent TLR4 antagonist for *in-vitro* and *in-vivo* applications. *Sci. Rep.* **6**, 34221 (2016).

80. Jin, X. *et al.* Advancements in understanding the molecular and immune mechanisms of *Bartonella* pathogenicity. *Front. Microbiol.* **14**, (2023).

81. Avila-Calderón, E. D. *et al.* Characterization of Outer Membrane Vesicles from *Brucella melitensis* and Protection Induced in Mice. *Clin. Dev. Immunol.* **2012**, (2012).

82. Liu, L. *et al.* Cell Type Dependent Suppression of Inflammatory Mediators by Myocardin Related Transcription Factors. *Front. Physiol.* **12**, 732564 (2021).

83. Tsukamoto, K. *et al.* The *Bartonella* autotransporter BafA activates the host VEGF pathway to drive angiogenesis. *Nat. Commun.* **11**, 3571 (2020).

84. Schulte, B. *et al. Bartonella quintana* Variably Expressed Outer Membrane Proteins Mediate Vascular Endothelial Growth Factor Secretion but Not Host Cell Adherence. *Infect. Immun.* **74**, 5003–5013 (2006).

85. Hayashi, K. *et al.* Role of CRP2-MRTF interaction in functions of myofibroblasts. *Cell Struct. Funct.* **48**, 83–98 (2023).

86. Arai, A., Spencer, J. A. & Olson, E. N. STARS, a Striated Muscle Activator of Rho Signaling and Serum Response Factor-dependent Transcription. *J. Biol. Chem.* **277**, 24453–24459 (2002).

87. Kuwahara, K., Barrientos, T., Pipes, G. C. T., Li, S. & Olson, E. N. Muscle-Specific Signaling Mechanism That Links Actin Dynamics to Serum Response Factor. *Mol. Cell. Biol.* **25**, 3173–3181 (2005).

88. Seeger, T. S. *et al.* Myozap, a Novel Intercalated Disc Protein, Activates Serum Response Factor–Dependent Signaling and Is Required to Maintain Cardiac Function In Vivo. *Circ. Res.* **106**, 880–890 (2010).

89. Rangrez, A. Y. *et al.* Dysbindin is a potent inducer of RhoA–SRF-mediated cardiomyocyte hypertrophy. *J. Cell Biol.* **203**, 643–656 (2013).

90. Rangrez, A. Y. *et al.* Myozap Deficiency Promotes Adverse Cardiac Remodeling via Differential Regulation of Mitogen-activated Protein Kinase/Serum-response Factor and β-Catenin/GSK-3β Protein Signaling. *J. Biol. Chem.* **291**, 4128–4143 (2016).

91. Selbach, M. *et al.* Host Cell Interactome of Tyrosine-Phosphorylated Bacterial Proteins. *Cell Host Microbe* **5**, 397–403 (2009).

92. Zhang, R., Liu, Q., Lyu, C., Gao, X. & Ma, W. Knockdown SENP1 Suppressed the Angiogenic Potential of Mesenchymal Stem Cells by Impacting CXCR4-Regulated MRTF-A SUMOylation and CCN1 Expression. *Biomedicines* **11**, 914 (2023).

93. Dehio, C. Molecular and Cellular Basis of *Bartonella* Pathogenesis. *Annu. Rev. Microbiol.* **58**, 365–390 (2004).

94. Zhu, C. *et al.* Soluble vascular endothelial growth factor (VEGF) receptor-1 inhibits migration of human monocytic THP-1 cells in response to VEGF. *Inflamm. Res.* **60**, 769–774 (2011).

95. Chai, J., Jones, M. K. & Tarnawski, A. S. Serum response factor is a critical requirement for VEGF signaling in endothelial cells and VEGF-induced angiogenesis. *FASEB J.* **18**, 1264–1266 (2004).

96. Zhang, L., Li, H.-L., Zhang, D.-D. & Cui, X.-C. Therapeutic effects of myocardin-related transcription factor A (MRTF-A) knockout on experimental mice with nonalcoholic steatohepatitis induced by high-fat diet. *Hum. Exp. Toxicol.* **40**, 1634–1645 (2021).

97. Yang, Y. *et al.* An Interplay Between MRTF-A and the Histone Acetyltransferase TIP60 Mediates Hypoxia-Reoxygenation Induced iNOS Transcription in Macrophages. *Front. Cell Dev. Biol.* **8**, 484 (2020).

98. Miller, T. *et al.* COMPASS: A complex of proteins associated with a trithorax-related SET domain protein. *Proc. Natl. Acad. Sci. U. S. A.* **98**, 12902–12907 (2001).

99. Takahashi, Y. *et al.* Structural analysis of the core COMPASS family of histone H3K4 methylases from yeast to human. *Proc. Natl. Acad. Sci.* **108**, 20526–20531 (2011).

100. Shu, X.-Z. *et al.* Histone acetyltransferase p300 promotes MRTF-A-mediated transactivation of VE-cadherin gene in human umbilical vein endothelial cells. *Gene* **563**, 17–23 (2015).

101. Lin, L., Zhang, Q., Fan, H., Zhao, H. & Yang, Y. Myocardin-Related Transcription Factor A Mediates LPS-Induced iNOS Transactivation. *Inflammation* **43**, 1351–1361 (2020).

102. Fang, F. *et al.* Myocardin-Related Transcription Factor A Mediates OxLDL-Induced Endothelial Injury. *Circ. Res.* **108**, 797–807 (2011).

103. Tian, W. *et al.* Myocardin-related transcription factor A (MRTF-A) plays an essential role in hepatic stellate cell activation by epigenetically modulating TGF-β signaling. *Int. J. Biochem. Cell Biol.* **71**, 35–43 (2016).

104. Facchetti, F. *et al.* Expression of Inducible Nitric Oxide Synthase in Human Granulomas and Histiocytic Reactions. *Am. J. Pathol.* **154**, 145–152 (1999).

105. Monteil, R. A. *et al.* Histological and ultrastructural study of one case of oral bacillary angiomatosis in HIV disease and review of the literature. *Eur. J. Cancer. B. Oral Oncol.* **30**, 65–71 (1994).

106. Yu, L. *et al.* Megakaryocytic Leukemia 1 Bridges Epigenetic Activation of NADPH Oxidase in Macrophages to Cardiac Ischemia-Reperfusion Injury. *Circulation* **138**, 2820–2836 (2018).

107. Al-Hetty, H. R. A. K. *et al.* SRF/MRTF-A and liver cirrhosis: Pathologic associations. *J. Dig. Dis.* **23**, 614–619 (2022).

108. Heerboth, S. *et al.* Use of Epigenetic Drugs in Disease: An Overview. *Genet. Epigenetics* **6**, 9–19 (2014).

Appendix

GGCCCCTCGAGATGCCACCGCTGAAGTCACCTGCAGCCTTCCACGAACAAAGGAGATCCCTCGAACGTGCGAGAACCGA
AGATTACCTTAAGAGGAAAATCAGAAGCAGACCCGAAAGGTCTGAACTCGTGAGAATGCATATCCTCGAGGAAACATCA
GCAGAACCCAGTCTGCAAGCAAAACAACTCAAACTCAAACGAGCTAGGCTGGCTGACGATCTGAACGAAAAGATCGCCC
AACGGCCAGGACCTATGGAACTCGTCGAAAAGAATATTCTGCCCGTAGAAAGCTCACTCAAAGAGGCGATTATCGTTGGT
CAAGTAAATTACCCAAAGGTTGCCGATTCTTCCTCATTTGACGAAGATTCCTCTGACGCACTGTCACCAGAACAACCCGCA
AGTCACGAATCTCAAGGATCCGTCCCTTCTCCACTTGAAGCGCGGGTGTCTGAGCCTCTTCTGTCCGCAACATCAGCGTCT
CCTACACAAGTGGTTAGTCAGCTCCCCATGGGGCGAGACTCTCGAGAGATGCTGTTTCTCGCTGAACAACCACCTCTCCC
GCCACCCCCACTCCTGCCGCCGTCTCTTACAAACGGGACTACAATTCCTACCGCGAAAAGTACTCCTACCCTGATCAAACA
GTCACAGCCAAAATCCGCTTCTGAAAAGAGCCAAAGGTCAAAGAAAGCAAAAGAATTGAAACCTAAAGTCAAGAAACTG
AAATACCATCAATACATTCCACCCGATCAAAAGCAAGATCGGGGAGCTCCACCTATGGATAGTAGCTATGCCAAAATTCT
CCAGCAACAACAGCTGTTTCTGCAACTTCAAATTTTGAATCAACAACAACAACAGCATCATAATTATCAAGCGATACTCCC
GGCACCACCTAAAAGCGCTGGAGAAGCTCTCGGTTCATCTGGTACGCCACCCGTGCGAAGTCTTTCTACAACAAACTCAT
CCAGCTCCAGCGGGGCACCAGGTCCTTGCGGCCTTGCTCGGCAAAATTCTACAAGTTTGACAGGAAAACCTGGTGCTTTG
CCCGCAAATTTGGATGATATGAAAGTAGCCGAACTCAAACAAGAATTGAAACTCCGGTCCCTGCCAGTGTCCGGGACAAA
GACAGAACTCATCGAACGGCTCAGGGCATACCAGGATCAGATTTCCCCAGTTCCTGGGGCTCCGAAAGCACCCGCGGCT
ACTTCCATACTCCATAAAGCCGGTGAAGTTGTCGTCGCTTTTCCCGCCGCTAGGTTGTCAACCGGTCCCGCATTGGTCGCC
GCCGGGCTTGCGCCGGCAGAAGTCGTTGTTGCTACTGTTGCATCATCAGGCGTCGTCAAATTCGGTTCCACCGGGTCAAC
ACCCCCAGTCTCCCCAACTCCATCCGAACGATCTCTCCTTTCCACTGGAGACGAGAATTCTACGCCAGGCGATACATTCGG
CGAAATGGTCACCAGCCCCCTTACCCAACTCACACTCCAAGCAAGCCCTCTTCAAATACTTGTCAAAGAAGAAGGACCAA
GAGCGGGATCTTGCTGTTTGTCCCCCGGTGGCCGAGCCGAACTTGAAGGCCGGGATAAAGATCAAATGCTTCAAGAAAA
GGATAAACAAATTGAAGCCCTTACCAGGATGTTGAGACAAAAGCAACAACTCGTAGAACGACTTAAACTCCAACTCGAAC
AAGAGAAACGCGCTCAACAACCGGCACCTGCTCCTGCACCACTTGGGACTCCAGTTAAACAAGAAAATTCTTTTAGCTCCT
GTCAATTGAGTCAACAACCTCTTGGACCAGCCCATCCCTTTAATCCATCCCTCGCTGCTCCCGCAACTAATCATATCGATCC
CTGCGCCGTAGCTCCTGGACCGCCCTCTGTTGTAGTCAAACAAGAGGCTCTTCAACCCGAACCAGAACCCGTGCCAGCAC
CTCAACTGCTGCTTGGACCACAAGGTCCGTCTCTGATTAAAGGTGTCGCTCCGCCTACTCTTATTACTGATTCTACGGGCA
CACATTTGGTACTTACTGTAACAAACAAGAACGCCGATTCCCCAGGGCTCAGCAGCGGAAGTCCACAACAACCTAGTTCA
CAACCAGGTAGCCCTGCCCCGGCACCAAGCGCACAAATGGATTTGGAACATCCGCTCCAACCACTTTTCGGCACTCCGAC
ATCCTTGCTTAAGAAAGAGCCACCCGGATACGAAGAGGCAATGTCCCAACAACCTAAGCAACAAGAGAACGGGAGTAGC
TCCCAACAAATGGATGATCTTTTCGATATACTGATACAATCTGGCGAGATCTCTGCTGACTTTAAAGAACCACCCAGCTTG
CCCGGTAAAGAAAAGCCTAGCCCTAAAACCGTGTGCGGTAGTCCATTGGCTGCGCAACCGTCTCCTTCCGCGGAACTTCC
ACAAGCGGCACCCCCACCACCGGGGAGTCCTAGCCTGCCGGGCCGGTTGGAAGATTTTCTTGAAAGTTCAACTGGTTTGC
CTCTCTTGACATCAGGACACGATGGCCCTGAACCACTGAGTCTGATAGATGATTTGCACTCCCAAATGCTCTCCTCTACAG
CTATACTCGATCATCCACCCAGCCCTATGGATACATCAGAGCTTCATTTCGTGCCAGAACCTTCCAGTACAATGGGACTTG
ATTTGGCCGACGGTCATTTGGATTCCATGGATTGGCTCGAATTGTCAAGTGGCGGCCCTGTCTTGTCACTGGCGCCTCTTT
CTACAACTGCACCGTCACTGTTTAGCACCGATTTTCTGGACGGTCACGATCTCCAACTCCATTGGGACAGCTGTCTGGATC
CGGGCCC

Appendix Figure 1: MAL DNA sequence. MAL DNA sequence synthesized by Twist Biosciences with the Kozak sequence shown in blue and the start codon shown in yellow. The sequence is shown (from top left) in the 5′ to 3′ direction.

1	MPPLKSPAAFHEQRRSLERARTEDYLKRKIRSRPERSELVRMHILEETSA	**50**
51	EPSLQAKQLKLKRARLADDLNEKIAQRPGPMELVEKNILPVESSLKEAII	**100**
101	VGQVNYPKVADSSSFDEDSSDALSPEQPASHESQGSVPSPLEARVSEPLL	**150**
151	SATSASPTQVVSQLPMGRDSREMLFLAEQPPLPPPPLLPPSLTNGTTIPT	**200**
201	AKSTPTLIKQSQPKSASEKSQRSKKAKELKPKVKKLKYHQYIPPDQKQDR	**250**
251	GAPPMDSSYAKILQQQQLFLQLQILNQQQQQHHNYQAILPAPPKSAGEAL	**300**
301	GSSGTPPVRSLSTTNSSSSSGAPGPCGLARQNSTSLTGKPGALPANLDDM	**350**
351	KVAELKQELKLRSLPVSGTKTELIERLRAYQDQISPVPGAPKAPAATSIL	**400**
401	HKAGEVVVAFPAARLSTGPALVAAGLAPAEVVVATVASSGVVKFGSTGST	**450**
451	PPVSPTPSERSLLSTGDENSTPGDTFGEMVTSPLTQLTLQASPLQILVKE	**500**
501	EGPRAGSCCLSPGGRAELEGRDKDQMLQEKDKQIEALTRMLRQKQQLVER	**550**
551	LKLQLEQEKRAQQPAPAPAPLGTPVKQENSFSSCQLSQQPLGPAHPFNPS	**600**
601	LAAPATNHIDPCAVAPGPPSVVVKQEALQPEPEPVPAPQLLLGPQGPSLI	**650**
651	KGVAPPTLITDSTGTHLVLTVTNKNADSPGLSSGSPQQPSSQPGSPAPAP	**700**
701	SAQMDLEHPLQPLFGTPTSLLKKEPPGYEEAMSQQPKQQENGSSSQQMDD	**750**
751	LFDILIQSGEISADFKEPPSLPGKEKPSPKTVCGSPLAAQPSPSAELPQA	**800**
801	APPPPGSPSLPGRLEDFLESSTGLPLLTSGHDGPEPLSLIDDLHSQMLSS	**850**
851	TAILDHPPSPMDTSELHFVPEPSSTMGLDLADGHLDSMDWLELSSGGPVL	**900**
901	SLAPLSTTAPSLFSTDFLDGHDLQLHWDSCLDPG **934**	

Appendix Figure 2: MAL amino acid sequence. Predicted MAL protein sequence (934 amino acids) based on the MAL DNA sequence shown in Appendix Figure 1. Red and green sequences correspond to RPEL and SAP domains in the MAL protein, respectively.